

Quantum Linear Time-Translation-Invariant Systems: Conjugate Symplectic Structure, Uncertainty Bounds, and Tomography

Jacques Ding,^{1,2,*} Hudson A. Loughlin,¹ and Vivishek Sudhir^{1,3,†}

¹*LIGO Laboratory, Massachusetts Institute of Technology, Cambridge, MA 02139*

²*Laboratoire Astroparticule et Cosmologie, Université Paris Cité, Paris, 75000, France*

³*Department of Mechanical Engineering, Massachusetts Institute of Technology, Cambridge, MA 02139*

(Dated: October 16, 2024)

Linear time-translation-invariant (LTI) models offer simple, yet powerful, abstractions of complex classical dynamical systems. Quantum versions of such models have so far relied on assumptions of Markovianity or an internal state-space description. We develop a general quantization scheme for multimode classical LTI systems that reveals their fundamental quantum noise, is applicable to non-Markovian scenarios, and does not require knowledge of an internal description. The resulting model is that of an open quantum LTI system whose dilation to a closed system is characterized by elements of the conjugate symplectic group. Using Lie group techniques, we show that such systems can be synthesized using frequency-dependent interferometers and squeezers. We derive tighter Heisenberg uncertainty bounds, which constrain the ultimate performance of any LTI system, and obtain an invariant representation of their output noise covariance matrix that reveals the ubiquity of “complex squeezing” in lossy systems. This frequency-dependent quantum resource can be hidden to homodyne and heterodyne detection and can only be revealed with more general “symplectodyne” detection. These results establish a complete and systematic framework for the analysis, synthesis, and measurement of arbitrary quantum LTI systems.

I. INTRODUCTION

A basic problem in science is to produce a “minimal” model of a “black box” system based on a set of response measurements on it. By a “black box”, we mean that the system is only accessible through a set of input and output ports. Finally, some principle of economy dictates what we mean by “minimal”. The model so inferred is the outcome of the scientific method applied to that system at the level of abstraction represented by the accessible ports. Systems theory formalizes the above task in the case where the system is classical. A high-point of this subject is the theory of linear time-translation-invariant (LTI) classical systems, which offers a simple and powerful framework to analyze [1–3] and synthesize [4–6] complex classical systems.

The purpose of this work is to present a framework for the analysis and synthesis of quantum LTI systems based only on their input-output description. Unlike a classical system, where consideration of noise is discretionary, any description of a quantum system has to contend with the unavoidable quantum noise in its accessible and inaccessible inputs. Quantum noises [7–10] furnish the appropriate mathematical model for the ubiquitous and fundamental noises afflicting all quantum systems. In essence, quantum systems are modeled as being driven by quantum noises. Thus, our task is to define and characterize the set of linear time-translation-invariant transformations on quantum noise, without invoking any further assumptions. In particular, we do not presume knowledge of an internal

description of the system, such as via a Hamiltonian, or quantum stochastic differential equations [8, 11–24]. Jettisoning that assumption makes our formalism more general — for example, it can be applied to systems that do not have a state-space description or are non-Markovian — and amenable to studying systems only based on what can be operationally verified about them. Effectively, we provide a scheme to quantize a given input-output model of a classical LTI system, and then to synthesize the resulting quantum description using commonly available laboratory elements.

Our formalism is pertinent in the study of complex systems that operate at the quantum-noise limit. For example, an element as simple and ubiquitous as an optical cavity involves a physical time delay, so that a Markovian state-space model [8] of it can be insufficient; such a lack is apparent in today’s most sensitive and complex quantum system [25].

Finally, our formalism is a generalization of techniques developed in Gaussian quantum information [26–30] in the sense that we study transformations of time-dependent Gaussian quantum stochastic processes. This is equivalent, as we will show, to the study of the group of frequency-dependent “conjugate symplectic” transformations which subsumes the oft-studied real symplectic group in Gaussian quantum information. To our knowledge, this is the first systematic study along these lines.

The rest of this paper is structured as follows. In Section II, we show how an input-output LTI model of a classical system can be promoted to a valid model of a quantum LTI system by adding appropriate noise modes. The resulting open quantum LTI system can be seen as a subsystems of a dilated closed quantum LTI system. In Section III, we show that closed quantum LTI systems are elements of the conjugate symplectic Lie group. We then

* ding@apc.in2p3.fr

† vivishek@mit.edu

use Lie group techniques to construct a one-parameter unitary representation of this group and show that arbitrary quantum LTI dynamics can be synthesized in terms of optical elements readily constructed in the lab. This parallels the solution of the classical synthesis problem [4–6] where a given classical LTI model is realized in terms of commonly available electrical elements. Section IV establishes tight uncertainty bounds for open and closed quantum LTI systems that are stricter than the usual Heisenberg uncertainty relation, and elucidates invariant properties of quantum noise in LTI systems. The latter generalizes the real-symplectic Williamson theorem [31] and identifies that quantum LTI systems generally exhibit “complex squeezing”, a quantum resource that is undetectable with homodyne or heterodyne detection, but can be observed with a more general “symplectodyne” detection [Section V]. Finally, in Section VI we explore the implications of the theory of quantum LTI systems developed in the preceding sections to the Schawlow-Townes limit in laser theory [32] and to quantum noise in gravitational wave detectors such as LIGO.

II. LTI TRANSFORMATIONS OF QUANTUM NOISE

A. Quantum LTI systems

We begin by studying “black box” systems with a known relationship between their inputs and outputs but without assuming any knowledge of their internal dynamics. We will show that by making the minimal assumptions of linearity and time-shift invariance, these systems are fully characterized by a set of “transfer functions” that dictate both their response to classical fields and to quantum noise.

To wit, consider a classical system that maps some set of n inputs, $\mathbf{x}^{\text{in}}(t) = \{x_i^{\text{in}}(t)\}_{i=1,\dots,n}$ to some set of m outputs $\mathbf{x}^{\text{out}}(t) = \{x_i^{\text{out}}(t)\}_{i=1,\dots,m}$ through a dynamical map \mathcal{G}^t at each time t via

$$\mathbf{x}^{\text{out}}(t) = \mathcal{G}^t[\mathbf{x}^{\text{in}}]. \quad (1)$$

As far as the input-output description is concerned, the system is the set of maps $\{\mathcal{G}^t\}$.

We now make two key assumptions: that the dynamical maps are *linear* and *time-translation invariant*. These notions are defined precisely as follows.

Definition 1. A classical system $\{\mathcal{G}^t\}$ is linear if

$$\mathcal{G}^t[\lambda\mathbf{x} + \lambda'\mathbf{x}'] = \lambda\mathcal{G}^t[\mathbf{x}] + \lambda'\mathcal{G}^t[\mathbf{x}']. \quad (2)$$

for all square-integrable functions \mathbf{x}, \mathbf{x}' and all constants λ, λ' at each instant t .

In general, a linear system’s map, \mathcal{G}^t from its n inputs to its m outputs can be decomposed in terms of a collection of maps, \mathcal{G}_{ij}^t from its j^{th} input port to its i^{th} output port (see Lemma 1).

Definition 2. Given the time-translation operator \mathcal{T}^s , defined by, $\mathcal{T}^s[f(t)] := f(t-s)$, the classical linear system $\{\mathcal{G}^t\}$ is said to be linear time-translation-invariant (LTI) if its dynamical map commutes with the time-translation operator, i.e.

$$(\mathcal{T}^s \circ \mathcal{G}_{ij}^t)[x] = (\mathcal{G}_{ij}^t \circ \mathcal{T}^s)[x], \quad (3)$$

for all inputs x , input and output ports, i, j , and times t, s .

The assumption of linearity is well-justified for a large class of systems since any system will respond approximately linearly to sufficiently small signals (as long as its dynamical map’s first derivatives with respect to these signals are non-vanishing, which defines the linear operating point). Systems that do not have an internal time reference, i.e. are autonomous in their internal mechanism, satisfy the assumption of time-translation invariance. Together, the LTI assumptions imply several key properties, of which the most pertinent is that the input-output response in Eq. (1) can be put in the form

$$\mathbf{x}^{\text{out}}[\omega] = \mathbf{G}[\omega]\mathbf{x}^{\text{in}}[\omega], \quad (4)$$

in terms of the Fourier transforms of the inputs and outputs (see Appendix B for a proof), and the transfer function matrix $\mathbf{G}[\omega]$ is uniquely related to $\{\mathcal{G}^t\}$.

To extend the notion of a LTI system from the classical to quantum domain, we note that inputs and outputs to a quantum system, in contrast to classical ones, need to be described by operator-valued stochastic processes. A convenient mathematical model is that of quantum noises defined as follows, and realized in practice by the quadratures of traveling electromagnetic fields [33], or voltages and currents in a transmission line [15, 34, 35], typically used to drive and probe quantum optical or electronic systems.

Definition 3. Quantum noises are pairs of operator-valued stochastic processes $\{\hat{q}_i(t), \hat{p}_i(t)\}_{i=1,\dots,m}$ that satisfy

$$\begin{aligned} [\hat{q}_i(t), \hat{q}_j(t')] &= 0 \\ [\hat{p}_i(t), \hat{p}_j(t')] &= 0 \\ [\hat{q}_i(t), \hat{p}_j(t')] &= i\delta_{ij}\delta(t-t'). \end{aligned} \quad (5)$$

By a quantum LTI system we have in mind the scenario depicted in Fig. 1: a set of n input ports and m output ports are accessible for classical response measurements — i.e. the inputs are driven by classical signals and their classical output response is measured; the observed classical response of the system satisfies the LTI assumptions in Eqs. (2) and (3), i.e.

$$\mathbf{x}^{\text{out}}(t) = \mathcal{G}^t[\mathbf{x}^{\text{in}}], \quad (6)$$

where $\mathbf{x} := \langle \hat{\mathbf{x}} \rangle$ denotes the expectation values of the input $\hat{\mathbf{x}}^{\text{in}}(t) := [\hat{q}_1^{\text{in}}(t), \dots, \hat{q}_n^{\text{in}}(t), \hat{p}_1^{\text{in}}(t), \dots, \hat{p}_n^{\text{in}}(t)]^T$ and output $\hat{\mathbf{x}}^{\text{out}}(t) := [\hat{q}_1^{\text{out}}(t), \dots, \hat{q}_m^{\text{out}}(t), \hat{p}_1^{\text{out}}(t), \dots, \hat{p}_m^{\text{out}}(t)]^T$. Since this definition only relies on the expectation values of

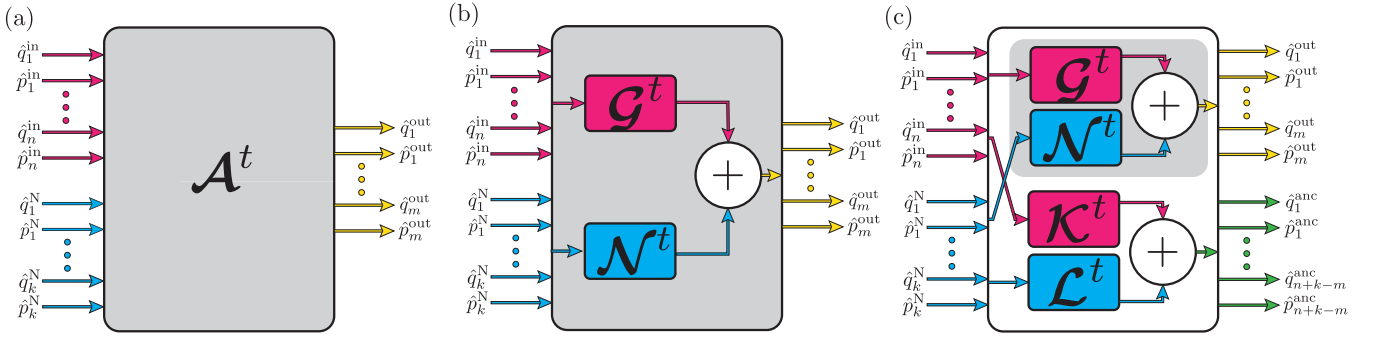


FIG. 1. *Quantum LTI System*. A quantum LTI system is described by n input quantum noises, which are mapped to m output quantum noises. (a) In general, a quantum LTI system will map n accessible inputs and k inaccessible inputs to its m outputs through a map \mathcal{A} . For a linear system, the maps from accessible and inaccessible inputs to outputs, \mathcal{G} and \mathcal{N} , can be considered separately as in (b) (see Eq. (7)). (c) By adding $n + k - m$ ancillary output modes (see Section II B) and the maps \mathcal{K} and \mathcal{L} from accessible and inaccessible inputs to ancillary outputs, the map \mathcal{A} can be dilated to a closed system (see Section II C).

quantum noises, we can determine whether a quantum system is LTI through classical measurements. Once a quantum system is verified to be LTI in this sense, the implications of classical systems theory apply to the above input-output equation. It can be put in the form of Eq. (4) which governs how the quantum LTI system maps its inputs to outputs *in expectation value only*. As a result, we can use a classical measurement to determine the transfer matrix $\mathcal{G}[\omega]$.

The analysis so far omits quantum fluctuations in the accessible inputs and in any inaccessible inputs. That is, Eq. (4) cannot tacitly be promoted to an operator relation (for example if $\{\mathcal{G}^t\}$ does not arise from unitary dynamics). The output (\mathbf{x}^{out}) can still be modeled as arising from the accessible (\mathbf{x}^{in}) and some additional inaccessible (\mathbf{x}^{N}) inputs, i.e. $\mathbf{x}^{\text{out}} = \mathcal{A}[\mathbf{x}^{\text{in}}, \mathbf{x}^{\text{N}}]$, where \mathcal{A} maps the accessible and inaccessible inputs to the accessible outputs. Assuming this map is linear, then

$$\mathbf{x}^{\text{out}} = \mathcal{A}[\mathbf{x}^{\text{in}}, 0] + \mathcal{A}[0, \mathbf{x}^{\text{N}}] =: \mathcal{G}[\mathbf{x}^{\text{in}}] + \mathcal{N}[\mathbf{x}^{\text{N}}], \quad (7)$$

where \mathcal{N} maps the inaccessible inputs to the accessible outputs. Further, if \mathcal{A} is assumed time-translation invariant, so is \mathcal{N} , and it admits a frequency domain representation just as \mathcal{G} does. Thus, Eq. (4) can be promoted to operator relations at the expense of adding additional quantum noises:

$$\hat{\mathbf{x}}^{\text{out}}[\omega] = \mathcal{G}[\omega]\hat{\mathbf{x}}^{\text{in}}[\omega] + \mathcal{N}[\omega]\hat{\mathbf{x}}^{\text{N}}[\omega] \quad (8)$$

where $\hat{\mathbf{x}}^{\text{N}}(t) := [\hat{q}_1^{\text{N}}(t), \dots, \hat{q}_k^{\text{N}}(t), \hat{p}_1^{\text{N}}(t), \dots, \hat{p}_k^{\text{N}}(t)]^T$ are k additional quantum noises with zero mean so that in an expectation value sense, Eq. (8) reduces to Eq. (4). We call \mathbf{x}^{N} “noise modes” to emphasize that their primary effect is to add noise in excess of what is conveyed by the accessible inputs alone. Figure 1(a,b) shows the relation between the linear map \mathcal{A} from all inputs to the accessible outputs and the maps \mathcal{G} from accessible inputs to accessible outputs and \mathcal{N} from inaccessible inputs to accessible outputs.

B. Quantum noise in LTI systems

Classical response measurements only reveal \mathcal{G} ; \mathcal{N} remains hidden since the ports corresponding to those inputs are inaccessible, i.e. the noise modes $\hat{\mathbf{x}}^{\text{N}}$ are internal to the system.

As we now show, even without an internal model of the system, it is possible to determine a class of hidden matrices \mathcal{N} that ensure the consistent mathematical description of the quantum LTI system. Further, as we will show, this class determines the *minimum* quantum noise that must be added given the accessible description of a quantum LTI system characterized by \mathcal{G} .

We require that the system’s output $\hat{\mathbf{x}}^{\text{out}}(t)$ obey the canonical commutation relations (CCR) in Eq. (5); in the frequency domain they read

$$\begin{aligned} [\hat{x}_i[\omega], \hat{x}_j[\omega']^\dagger] &= 2\pi i \delta[\omega - \omega'] J_{ij}^{\text{out}}, \\ \text{where } \mathbf{J}^{\text{out}} &:= \begin{bmatrix} \mathbf{0}_m & \mathbf{1}_m \\ -\mathbf{1}_m & \mathbf{0}_m \end{bmatrix} \end{aligned} \quad (9)$$

is the $2m$ -dimensional symplectic matrix of the m output modes, given in terms of $\mathbf{1}_m$ and $\mathbf{0}_m$, the m -dimensional identity and zero matrices respectively. Stipulating that the outputs are given by the system’s input-output relation [Eq. (8)] then implies that

$$\mathcal{N}[\omega]i\mathbf{J}^{\text{N}}\mathcal{N}[\omega]^\dagger = i\mathbf{J}^{\text{out}} - \mathcal{G}[\omega]i\mathbf{J}^{\text{in}}\mathcal{G}[\omega]^\dagger, \quad (10)$$

where \mathbf{J}^{in} , \mathbf{J}^{N} are respectively the $2n$ and $2k$ dimensional symplectic matrices corresponding to the inputs and noise modes respectively. Equation (10) is sufficient to determine the mathematical consistency of any hidden transfer matrix \mathcal{N} .

Since the left and right hand sides of Eq. (10) are both Hermitian, they can be unitarily diagonalized at every

frequency as

$$i\mathbf{J}^{\text{out}} - \mathbf{G}[\omega]i\mathbf{J}^{\text{in}}\mathbf{G}[\omega]^\dagger = \mathbf{U}[\omega] \begin{bmatrix} \mathbf{D}^+[\omega] & \mathbf{0} & \mathbf{0} \\ \mathbf{0} & \mathbf{D}^-[\omega] & \mathbf{0} \\ \mathbf{0} & \mathbf{0} & \mathbf{0} \end{bmatrix} \mathbf{U}[\omega]^\dagger, \quad (11)$$

where $\mathbf{D}^+[\omega]$ and $\mathbf{D}^-[\omega]$ are diagonal matrices with only positive and negative entries respectively. In general, \mathbf{D}^+ and \mathbf{D}^- can have different dimensions; we denote $d_\pm := \dim(\mathbf{D}^\pm[\omega])$. This dimension determines the minimum number of noise modes as per the following theorem (see SI Section I for the proof).

Theorem 1. *The minimum number of noise modes for a quantum LTI system that satisfies Equation (10) is $\ell = \max(d_-, d_+)$.*

While Eq. (10) cannot be satisfied with fewer than ℓ noise modes, it can always be satisfied by adding more than ℓ noise modes, or example by taking the minimal-noise construction and adding amplifiers and attenuators in series, or by decomposing a single loss as a series of losses. Thus, the bound in Theorem 1 is tight.

In the case that we add exactly ℓ noise modes, the matrix $\mathbf{N}[\omega]$ is given by

$$\mathbf{N}[\omega] = \mathbf{U}[\omega]\mathbf{\Gamma}[\omega]\mathbf{P}^\dagger, \quad (12)$$

where $\mathbf{\Gamma}[\omega] = \{\gamma_i[\omega]\delta_{ij}\}$ is a $m \times k$ matrix with diagonal entries

$$\gamma_i = \begin{cases} \sqrt{D_{ii}^+}, & \text{if } 1 \leq i \leq d_+ \\ \sqrt{|D_{ii}^-|}, & \text{if } d_+ + 1 \leq i \leq d_+ + d_- \\ 0, & \text{otherwise} \end{cases} \quad (13)$$

and all other entries zero, and \mathbf{P} is the unitary matrix that diagonalizes $i\mathbf{J}^{\text{N}}$. Note that γ_i are the singular values of \mathbf{N} . These should be ordered such that the singular values determined by \mathbf{D}^+ multiply +1 in the diagonalization of $i\mathbf{J}^{\text{N}}$ and the singular values determined by \mathbf{D}^- multiply -1.

If $\mathbf{G}[\omega]$ and $\mathbf{N}[\omega]$ are frequency-independent [27, 28], their entries must be real-valued (this follows from the fact that each component of $\mathbf{x}(t)$ is Hermitian, i.e. $\hat{x}_i[\omega]^\dagger = \hat{x}_i[-\omega]$). In this case, both the left and right-hand sides of Eq. (10) are Hermitian and anti-symmetric, so their eigenvalues must be real-valued and come in positive and negative pairs, implying $d_+ = d_-$, and so the minimum number of added noise modes is $\ell = d_\pm$. That is, in the frequency-independent case, at most the same number of noise modes must be added as there are outputs. By contrast, in the frequency-dependent case, up to twice as many noise modes as outputs need to be added.

We will return to the important question of how to quantify the added noise at the accessible outputs of the system, the minimum added noise, and any trade-offs therein, in Section IV.

C. Dilation of a quantum LTI system

The quantum system resulting from the addition of noise modes is still not unitary. A necessary condition to realize a unitary system is that the total number of inputs and outputs be equal. The quantum LTI system in Eq. (8) can be enlarged, or dilated, into the form (shown in Fig. 1c)

$$\begin{bmatrix} \hat{\mathbf{x}}^{\text{out}}[\omega] \\ \hat{\mathbf{x}}^{\text{anc}}[\omega] \end{bmatrix} = \begin{bmatrix} \mathbf{G}[\omega] & \mathbf{N}[\omega] \\ \mathbf{K}[\omega] & \mathbf{L}[\omega] \end{bmatrix} \begin{bmatrix} \hat{\mathbf{x}}^{\text{in}}[\omega] \\ \hat{\mathbf{x}}^{\text{N}}[\omega] \end{bmatrix}, \quad (14)$$

which includes ancillary outputs ($\hat{\mathbf{x}}^{\text{anc}}$) so as to ensure that the total number of outputs equals the total number of inputs. Here, $\hat{\mathbf{x}}^{\text{in}}$, $\hat{\mathbf{x}}^{\text{out}}$ are the system's accessible inputs and outputs, while $\hat{\mathbf{x}}^{\text{N}}$, $\hat{\mathbf{x}}^{\text{anc}}$ are the system's inaccessible, or unobserved, inputs and outputs. The matrices \mathbf{K} and \mathbf{L} represent the LTI maps \mathcal{K} and \mathcal{L} that respectively map the system's accessible and inaccessible inputs to its inaccessible outputs, as depicted in Fig. 1.

Importantly, by construction, the matrix

$$\mathbf{M}^{\text{ext}}[\omega] := \begin{bmatrix} \mathbf{G}[\omega] & \mathbf{N}[\omega] \\ \mathbf{K}[\omega] & \mathbf{L}[\omega] \end{bmatrix} \quad (15)$$

is square, and the dilated input-output relation in Eq. (14) can be cast into the form

$$\hat{\mathbf{y}}^{\text{out}}[\omega] = \mathbf{M}^{\text{ext}}[\omega]\hat{\mathbf{y}}^{\text{in}}[\omega], \quad (16)$$

of which, the system given in Eq. (8) (and shown in Fig. 1b) is an open subsystem. As before, the inputs and outputs of this dilated system must satisfy the CCRs, which implies that

$$\mathbf{M}^{\text{ext}}[\omega]\mathbf{J}^{\text{ext}}\mathbf{M}^{\text{ext}}[\omega]^\dagger = \mathbf{J}^{\text{ext}} \quad (17)$$

where

$$\mathbf{J}^{\text{ext}} := \begin{bmatrix} \mathbf{J}_{2n \times 2n} & \mathbf{0} \\ \mathbf{0} & \mathbf{J}_{2k \times 2k} \end{bmatrix}. \quad (18)$$

Any square matrix \mathbf{M}^{ext} that satisfies Eq. (17) forms a group — the conjugate symplectic group. This group plays a key role in the study of frequency-dependent transformations of quantum noise, and subsumes the symplectic group that arises in the study of Gaussian quantum random variables. The following section explicates the relevant properties of the conjugate symplectic group. In particular, Eq. (17) is sufficient to ensure that the dilated input-output relation in Eq. (16) arises from reversible and therefore unitary, but not necessarily Markovian, quantum dynamics.

The outstanding question in the construction of the dilated system described by \mathbf{M}^{ext} [Eq. (15)] is whether, given the matrices \mathbf{G} , \mathbf{N} (the latter possibly constructed from the former via the procedure in Section II B), it is always possible to find \mathbf{K} , \mathbf{L} that enable a unitary dilation. A conjugate-symplectic diagonalization procedure, extending a result in the frequency-independent case [36],

shows that it is always possible to find \mathbf{K}, \mathbf{L} for a unitary dilation (see SI Section II) [37]. In effect, any LTI system can be thought of as a subsystem of a dilated unitary system governed by Eq. (16) with some of the output modes ($\hat{\mathbf{x}}^{\text{anc}}$) inaccessible.

III. CONJUGATE SYMPLECTIC GROUP

Following the discussion so far, it is sufficient to study a quantum LTI “black box” with n input quantum noises $\hat{\mathbf{x}}^{\text{in}}(t)$ and n outputs $\hat{\mathbf{x}}^{\text{out}}(t)$, with the complex-valued transfer function matrix $\mathbf{M}[\omega]$ that describes the input-output relation

$$\hat{\mathbf{x}}^{\text{in}}[\omega] \mapsto \hat{\mathbf{x}}^{\text{out}}[\omega] = \mathbf{M}[\omega]\hat{\mathbf{x}}^{\text{in}}[\omega]. \quad (19)$$

Recall that we assume only the following minimal hypotheses: (i) the quantum noises are hermitian, i.e. $\hat{x}_i^\dagger(t) = \hat{x}_i(t)$, for all $i \in \{1, \dots, 2n\}$; and, (ii) they satisfy the canonical commutation relations given in Eq. (5). The first condition implies that

$$\mathbf{M}[\omega]^* = \mathbf{M}[-\omega]; \quad (20)$$

in particular $\mathbf{M}[0] \in \mathcal{M}_{2n}(\mathbb{R})$, i.e. it is a $2n$ -dimensional real matrix. The second condition implies that

$$\mathbf{M}[\omega] \mathbf{J} \mathbf{M}[\omega]^\dagger = \mathbf{J} \quad (21)$$

where \mathbf{J} is the $2n$ -dimensional symplectic matrix. These physical requirements motivate the following mathematical definition of the conjugate symplectic group [38].

Definition 4. *The conjugate symplectic group of order $2n$ is the set*

$$\text{Sp}^\dagger(2n) := \left\{ \mathbf{M} \in \mathcal{M}_{2n}(\mathbb{C}) \mid \mathbf{M} \mathbf{J} \mathbf{M}^\dagger = \mathbf{J} \right\}. \quad (22)$$

where \mathbf{J} is the $2n$ -dimensional symplectic matrix.

That the set $\text{Sp}^\dagger(2n)$ is a group can be directly verified (using the fact that $\mathbf{J}^\dagger = \mathbf{J}^{-1} = -\mathbf{J}$). In fact, the transfer matrix $\mathbf{M}[\omega]$ at each frequency is an element of the conjugate symplectic group. It can be verified that the condition in Eq. (20) is compatible with the group structure, i.e. if $\mathbf{M}[\omega]$ is conjugate symplectic, then so is $\mathbf{M}[-\omega]^*$. Thus, Eq. (20) may be viewed as defining the negative-frequency extension of the conjugate symplectic, positive-frequency transfer matrix.

The group structure implies in particular that if $\mathbf{M}[\omega]$ is conjugate symplectic, so is $\mathbf{M}^{-1}[\omega]$; i.e. the input-output relation in Eq. (19) is reversible [39]. This reversibility suggests that any transfer function matrix can be implemented unitarily. We construct the unitary implementation in Section III A and its synthesis — using common laboratory optical elements — in Section III B.

A. One-parameter unitary representation

In order to construct a unitary representation of $\text{Sp}^\dagger(2n)$ in the Hilbert space \mathcal{H} of the quantum noises, we pass through the Lie algebra $\text{sp}^\dagger(2n)$. In what follows, we suppress the frequency argument unless required.

In general, for matrix Lie groups with coefficients in \mathbb{R} or \mathbb{C} , the algebra is the tangent space at the identity element $\mathbf{1}$ of the group. Let $\tau \mapsto \mathbf{M}_\tau$ be a continuous map from the reals $\{\tau\} = \mathbb{R}$ to the group such that $\mathbf{M}_0 = \mathbf{1}$. The group property implies that $\mathbf{M}_\tau = (\mathbf{M}_{\tau/m})^m$ for any integer m . In the neighborhood of the identity, $\mathbf{M}_\tau \stackrel{\tau \rightarrow 0}{\approx} \mathbf{1} + \tau \mathbf{\Lambda}$, where $\mathbf{\Lambda} \in \mathcal{M}_{2n}(\mathbb{C})$ is the generator of the algebra [40].

The group element can then be expressed in terms of the generator:

$$\mathbf{M}_\tau = \lim_{m \rightarrow \infty} (\mathbf{M}_{\tau/m})^m \approx \lim_{m \rightarrow \infty} \left(\mathbf{1} + \frac{\tau}{m} \mathbf{\Lambda} \right)^m = e^{\tau \mathbf{\Lambda}}.$$

Since the generator needs to generate the group in question, $\mathbf{M}_\tau \mathbf{J} \mathbf{M}_\tau^\dagger = \mathbf{J}$; taking the derivative of this relation at $\tau = 0$ gives $\mathbf{\Lambda} \mathbf{J} = (\mathbf{\Lambda} \mathbf{J})^\dagger$, which defines the conjugate symplectic algebra [41].

Definition 5. *The conjugate symplectic Lie algebra of order $2n$ is the set*

$$\text{sp}^\dagger(2n) := \{ \mathbf{\Lambda} \in \mathcal{M}_{2n}(\mathbb{C}) \mid \mathbf{\Lambda} \mathbf{J} \text{ is hermitian} \}. \quad (23)$$

In order to imbue physical meaning into this description, we now look for a unitary representation of $\text{Sp}^\dagger(2n)$. This means a map

$$\begin{aligned} \text{Sp}^\dagger(2n) &\rightarrow \mathcal{H} \\ \mathbf{M} &\mapsto \hat{U}(\mathbf{M}), \end{aligned} \quad (24)$$

that is unitary, i.e. $\hat{U}(\mathbf{M})^\dagger \hat{U}(\mathbf{M}) = \hat{\mathbf{1}}$, and respects the group structure, i.e. $\hat{U}(\mathbf{M} \mathbf{M}') = \hat{U}(\mathbf{M}) \hat{U}(\mathbf{M}')$. Arguments similar to the one above can be deployed on the representation. To wit, the group identity is mapped to the identity element in Hilbert space, and so in the neighborhood of the identity, $\hat{U}(\mathbf{M}_\tau) \stackrel{\tau \rightarrow 0}{\approx} \hat{U}(\mathbf{1} + i\tau \mathbf{\Lambda}) \approx \hat{\mathbf{1}} + i\tau \hat{H}(\mathbf{\Lambda})$; here $\mathbf{\Lambda} \mapsto \hat{H}(\mathbf{\Lambda})$ is a representation of the algebra $\text{sp}^\dagger(2n)$ on the Hilbert space. By the representation property, $\hat{U}(\mathbf{M}_\tau) = \hat{U}(\mathbf{M}_{\tau/m})^m$ for any $m \in \mathbb{N}$; using the infinitesimal form above, and taking the limit $m \rightarrow \infty$ then gives $\hat{U}(\mathbf{M}_\tau) = \exp[i\tau \hat{H}(\mathbf{\Lambda})]$. For \hat{U} to be unitary, $\hat{H}(\mathbf{\Lambda})$ has to be hermitian [42].

The point of the unitary representation is that the transformation \mathbf{M}_τ must be expressible as:

$$\hat{x}_j \mapsto \hat{x}'_j = (\mathbf{M}_\tau)_{jk} \hat{x}_k = \hat{U}(\mathbf{M}_\tau)^\dagger \hat{x}_j \hat{U}(\mathbf{M}_\tau). \quad (25)$$

Evaluating these two expressions for an infinitesimal transformation gives (restoring the frequency arguments)

$$-i[\hat{H}(\mathbf{\Lambda}), \hat{x}_j[\omega]] = \Lambda_{jk}[\omega] \hat{x}_k[\omega], \quad (26)$$

which determines $\hat{H}(\mathbf{\Lambda})$ for a given $\mathbf{\Lambda}$. The solution is

$$\begin{aligned}\hat{H}(\mathbf{\Lambda}) &= \frac{1}{2} \int \hat{x}_i[\omega] J_{ij} \Lambda_{jk}[\omega] \hat{x}_k[\omega] \frac{d\omega}{2\pi} \\ &= \frac{1}{2} \int \hat{x}_i(t) J_{ij} \Lambda_{jk}(t-t') \hat{x}_k(t') dt dt'.\end{aligned}\quad (27)$$

From the perspective of quantum mechanics, $\hat{U}(\mathbf{M})$ is the unitary operator that realizes the dynamics represented by the black box transfer matrix \mathbf{M} ; then, $\hat{H}(\mathbf{\Lambda})$, being the hermitian generator of the unitary, is the Hamiltonian. Its form can be interpreted as the input quantum noise \hat{x}_i^{in} at time t interacting with \hat{x}_k^{in} at time t' with the coupling constant $J_{ij} \Lambda_{jk}(t-t')$. That is, the interaction is delocalized in time, encoding the potential non-Markovian character of the dynamics. The Markovian limit corresponds to $\Lambda_{jk}(t-t') = \Lambda_{jk} \delta(t-t')$.

Theorem 2 (Optical decomposition of $\text{Sp}^\dagger(2n)$). *Any $\mathbf{M} \in \text{Sp}^\dagger(2n)$ can be uniquely factorized as*

$$\mathbf{M} = \begin{bmatrix} \mathbf{V}_1 & \mathbf{0} \\ \mathbf{0} & \mathbf{V}_1 \end{bmatrix} \begin{bmatrix} \mathbf{C}_1 & -\mathbf{S}_1 \\ \mathbf{S}_1 & \mathbf{C}_1 \end{bmatrix} \begin{bmatrix} \mathbf{W}_1 & \mathbf{0} \\ \mathbf{0} & \mathbf{W}_1 \end{bmatrix} \begin{bmatrix} \mathbf{D} & \mathbf{0} \\ \mathbf{0} & \mathbf{D}^{-1} \end{bmatrix} \begin{bmatrix} \mathbf{W}_2 & \mathbf{0} \\ \mathbf{0} & \mathbf{W}_2 \end{bmatrix} \begin{bmatrix} \mathbf{C}_2 & -\mathbf{S}_2 \\ \mathbf{S}_2 & \mathbf{C}_2 \end{bmatrix} \begin{bmatrix} \mathbf{V}_2 & \mathbf{0} \\ \mathbf{0} & \mathbf{V}_2 \end{bmatrix}, \quad (28)$$

where $\mathbf{V}_i, \mathbf{W}_i \in U(n)$; $\mathbf{C}_i = \text{diag}(\cos \theta_{1,i}, \dots, \cos \theta_{n,i})$, $\mathbf{S}_i = \text{diag}(\sin \theta_{1,i}, \dots, \sin \theta_{n,i})$, with $\theta_{k,i} \in \mathbb{R}$; and, $\mathbf{D} = \text{diag}(e^{r_1}, \dots, e^{r_n})$ with $r_k \in \mathbb{R}$. Without loss of generality, for each of the $\mathbf{V}_1, \mathbf{V}_2, \mathbf{W}_1$ matrices, n phases among their independent matrix coefficients can be fixed.

The physical import of this result is that any transfer function $\mathbf{M}[\omega]$ can be implemented as a succession of a n -mode frequency-dependent Mach-Zehnder, a set of frequency-dependent single mode squeezers, and another n -mode frequency-dependent Mach-Zehnder, as shown in Fig. 2. To realize a n -mode frequency dependent Mach-Zehnder, it suffices to apply the algorithm outlined in the frequency-independent case [47, 48] with frequency-dependent phase-shifters and beam-splitters, both of which can be realized by detuning an optical cavity.

Theorem 2 is a generalization of two central results in synthesis in two different fields of study. On the one hand, in quantum optics of frequency-independent modes, it is a generalization of the fact that a real symplectic transformation of n modes can be decomposed into a set of n single-mode squeezers sandwiched between two n -mode Mach-Zehnder interferometers [26, 30, 43, 49], where the latter can be implemented using a set of two-mode beam-splitters and phase shifters [47, 48]. On the other hand, it is the natural generalization of the classical theory of electrical network synthesis [4–6]; the subject of this theory is to synthesize an electrical network whose response matches that of a specified “realizable” transfer function. The fundamental difficulty in that realm is to ensure good impedance match between the various stages

B. Synthesis of $\text{Sp}^\dagger(2n)$ transformation

The Hamiltonian formally conveys the microscopic structure of the interactions within the black box, but it does not directly inform how a given transfer matrix $\mathbf{M}[\omega]$ may be synthesized in practice in a lab.

Any synthesis procedure is the result of factorizing a given $\mathbf{M} \in \text{Sp}^\dagger(2n)$ in terms of other elements of the conjugate symplectic group, so that each factor can be physically realized. We prove that such a factorization can be achieved by first using a conjugate symplectic singular value decomposition [44, 45], which decomposes \mathbf{M} into a product of elements of $\text{Sp}^\dagger(2n) \cap U(2n)$ and a positive repeating diagonal matrix, followed by a “cosine” decomposition in $\text{Sp}^\dagger(2n) \cap U(2n)$. The resulting factorization, which we call the “optical decomposition”, is as follows. (See Supplementary Information Section III for the proof, and a sketch of its relation to the “KAK” decomposition in the theory of Lie groups [46].)

whose cascade forms the full network; if not, succeeding stages load the preceding ones. The quantum analog of such loading is back-action [50]. So in a practical implementation, stringent control of extraneous back-action, such as back-scatter in an optical implementation, will need to be exercised.

C. Related descriptions of linear quantum systems

The LTI transformation of the quantum noises can be equivalently described in terms of the creation/annihilation operators $\hat{\mathbf{a}}(t) := [\hat{a}_1(t), \dots, \hat{a}_n(t), \hat{a}_1^\dagger(t), \dots, \hat{a}_n^\dagger(t)]^\top$, where $\hat{a}_i(t) := (\hat{q}_i(t) + i\hat{p}_i(t))/\sqrt{2}$. Since this transformation $\hat{\mathbf{x}} \mapsto \hat{\mathbf{a}} = \mathbf{P}^\dagger \hat{\mathbf{x}}$ is implemented by the unitary matrix

$$\mathbf{P} := \frac{1}{\sqrt{2}} \begin{bmatrix} \mathbf{1}_n & \mathbf{1}_n \\ -i\mathbf{1}_n & i\mathbf{1}_n \end{bmatrix}, \quad (29)$$

the LTI transformation $\hat{\mathbf{x}}_{\text{in}}[\omega] \mapsto \hat{\mathbf{x}}_{\text{out}}[\omega] = \mathbf{M}[\omega] \hat{\mathbf{x}}_{\text{in}}[\omega]$, induces the LTI transformation on creation/annihilation operators, $\hat{\mathbf{a}}_{\text{in}}[\omega] \mapsto \hat{\mathbf{a}}_{\text{out}}[\omega] = (\mathbf{P}^\dagger \mathbf{M}[\omega] \mathbf{P}) \hat{\mathbf{a}}_{\text{in}}[\omega]$. The former transformation preserves the CCR in Eq. (5), whereas the latter transformation preserves the CCR

$$[\hat{\mathbf{a}}_j[\omega], \hat{\mathbf{a}}_k[\omega']^\dagger] = 2\pi\delta[\omega - \omega'] (\mathbf{I}_n)_{jk}, \quad (30)$$

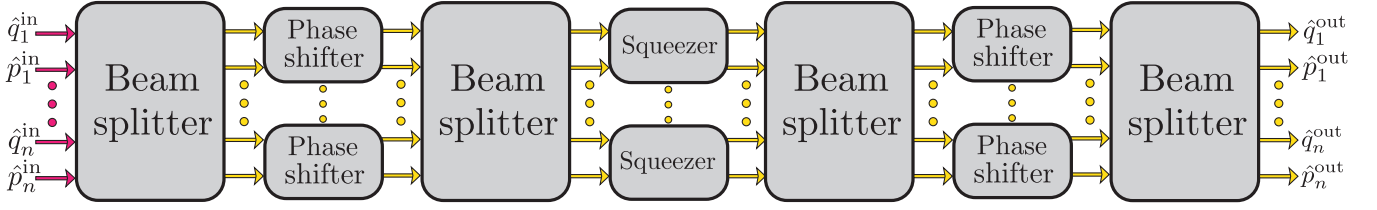


FIG. 2. Optical decomposition (Theorem 2) of a frequency-dependent LTI quantum system. While formally similar to the Bloch-Messiah decomposition on the real symplectic group $\text{Sp}(2n, \mathbb{R})$ [43], note that each component is a function of frequency and the beam-splitter component is complex-valued.

where $\mathbf{I}_n := \mathbf{P}^\dagger \mathbf{J}_{2n} \mathbf{P} = \text{diag}(\mathbf{1}_n, -\mathbf{1}_n)$. This motivates the following definition.

Definition 6. *The indefinite unitary group of signature (n, m) is the set*

$$U(n, m) := \left\{ \mathbf{A} \in \mathcal{M}_{n+m}(\mathbb{C}) \mid \mathbf{A} \mathbf{I}_{n,m} \mathbf{A}^\dagger = \mathbf{I}_{n,m} \right\} \quad (31)$$

where $\mathbf{I}_{n,m} = \text{diag}(\mathbf{1}_n, -\mathbf{1}_m)$; we denote $\mathbf{I}_n = \mathbf{I}_{n,n}$.

The group $U(n, n)$ then describes CCR-preserving LTI transformations of the creation/annihilation operators, and we have the group isomorphism $\text{Sp}^\dagger(2n) \cong U(n, n)$, realized by the map $\mathbf{M} \mapsto \mathbf{P}^\dagger \mathbf{M} \mathbf{P}$.

The oft-studied real symplectic group [26–28, 30, 51] of order $2n$, $\text{Sp}(2n, \mathbb{R})$, emerges from the conjugate symplectic order $\text{Sp}^\dagger(2n)$ in one of two different ways.

In the frequency-independent case, $\mathbf{M}[\omega] = \mathbf{M}[0]$; the symmetry property [Eq. (20)] $\mathbf{M}[\omega]^* = \mathbf{M}[-\omega]$ then implies that $\mathbf{M} := \mathbf{M}[0]$ is real-valued. Thus the conjugate symplectic condition [Eq. (21)] reduces to $\mathbf{M} \mathbf{J} \mathbf{M}^T = \mathbf{J}$, i.e. $\mathbf{M} \in \text{Sp}(2n, \mathbb{R})$ in the frequency-independent case, and so $\text{Sp}(2n, \mathbb{R}) \subset \text{Sp}^\dagger(2n)$.

More generally, the operators

$$\hat{x}_\mu := \int f_{\mu i}(t) \hat{x}_i(t) dt = \int f_{\mu i}^*[\omega] \hat{x}_i[\omega] \frac{d\omega}{2\pi}, \quad (32)$$

defined by sampling the quantum noise with the real-valued “window” functions $\{f_{\mu i}(t)\}$ which satisfy $\int f_{\mu i}(t) f_{\nu j}(t) dt = \delta_{\mu i} \delta_{\nu j}$, are canonically conjugate variables of a set of harmonic oscillators, i.e. $[\hat{x}_\mu, \hat{x}_\nu] = iJ_{\mu\nu}$.

A CCR-preserving LTI transformation of the quantum noises $\{\hat{x}_i[\omega]\}$ induces a CCR-preserving (i.e. canonical) linear transformation of $\{\hat{x}_\mu\}$. The latter forms the group $\text{Sp}(2n, \mathbb{R})$; but since the map Eq. (32) is many-to-one, it realizes the inclusion $\text{Sp}(2n, \mathbb{R}) \subset \text{Sp}^\dagger(2n)$. The physical interpretation of sampling is useful in defining harmonic oscillator modes out of propagating quantum optical fields [29, 33, 52]; we will revisit this aspect in Section V in the context of characterizing a quantum LTI system.

The reason that the conjugate symplectic group is fundamentally distinct from the real symplectic group is that the former describes linear transformations of the *non-hermitian* operators $\hat{\mathbf{x}}[\omega] = [\hat{\mathbf{q}}[\omega], \hat{\mathbf{p}}[\omega]]^T$. This can be

ameliorated by defining, for $\omega \geq 0$, the set of $4n$ hermitian operators

$$\hat{\mathfrak{X}}[\omega] = \frac{1}{\sqrt{2}} \begin{bmatrix} \hat{\mathbf{x}}[+\omega] + \hat{\mathbf{x}}[-\omega] \\ -i(\hat{\mathbf{x}}[+\omega] - \hat{\mathbf{x}}[-\omega]) \end{bmatrix} = \mathbb{P} \begin{bmatrix} \hat{\mathbf{x}}[+\omega] \\ \hat{\mathbf{x}}[-\omega] \end{bmatrix}; \quad (33)$$

here \mathbb{P} is the $4n$ -dimensional unitary matrix that performs the required linear transformation. Partitioned into the form $\hat{\mathfrak{X}}[\omega] = [\hat{\mathbf{x}}^A[\omega], \hat{\mathbf{x}}^B[\omega]]$, these are precisely the “two-photon quadratures” in the Caves-Schumaker formalism [53–58]. Importantly, $\hat{x}_i^{A,B}[\omega]$ are all hermitian and are canonically conjugate of each other: $[\hat{q}_j^A[\omega], \hat{p}_k^A[\omega']] = 2\pi i \delta_{jk} \delta[\omega - \omega']$ (similarly for the \mathbf{B} quadratures). Thus, the set of CCR-preserving linear transformations acting on $\hat{\mathfrak{X}}[\omega]$ is the real symplectic group $\text{Sp}(4n, \mathbb{R})$ for $2n$ modes. However, such transformations generally mix $\hat{\mathbf{x}}[+\omega]$ and $\hat{\mathbf{x}}[-\omega]$, indicating that they cannot arise from LTI transformations of $\hat{\mathbf{x}}[\omega]$. Indeed the LTI transformation $\hat{\mathbf{x}}[\omega] \mapsto \mathbf{M}[\omega] \hat{\mathbf{x}}[\omega]$ — the totality of which form the conjugate symplectic group $\text{Sp}^\dagger(2n)$ — induces the transformation $\hat{\mathfrak{X}}[\omega] \mapsto \mathbb{P} \text{diag}(\mathbf{M}[\omega], \mathbf{M}[-\omega]) \mathbb{P}^\dagger \hat{\mathfrak{X}}[\omega]$, which is clearly a subgroup of $\text{Sp}(4n, \mathbb{R})$ (see Section IV of SI for proofs). Thus follows the inclusion $\text{Sp}^\dagger(2n) \subset \text{Sp}(4n, \mathbb{R})$.

In sum, the conjugate symplectic group of order $2n$ — describing the LTI transformations of quantum white noise — encompasses the set of linear canonical transformations of harmonic oscillator modes — the subject of Gaussian quantum information studies — and is included in the set of linear “two-photon” transformations, i.e.

$$\text{Sp}(2n, \mathbb{R}) \subset \text{Sp}^\dagger(2n) \cong U(n, n) \subset \text{Sp}(4n, \mathbb{R}). \quad (34)$$

IV. UNCERTAINTY PRINCIPLES FOR QUANTUM LTI SYSTEMS

Given the black-box transfer matrix $\mathbf{M}[\omega]$ of a quantum LTI system — either closed, in which case $\mathbf{M} \in \text{Sp}^\dagger$, or open, in which case hidden noise modes are present — the unavoidable implication of quantum mechanics is that the outputs feature a certain minimum noise. In the following, we elucidate the structure and trade-off among the uncertainties in the quantum noises.

We assume that the quantum noises are weak-stationary, i.e. $\langle \hat{x}_i(t) \hat{x}_j(t') \rangle = \langle \hat{x}_i(t-t') \hat{x}_j(0) \rangle$ for all

quantum noises and times t, t' . This assumption is consistent in the sense that an LTI map preserves the weak-stationary property of inputs. Then the fluctuations in the $2n$ quantum noises $\hat{\mathbf{x}}(t)$ are described by the (symmetrized) spectral density matrix (SDM) $\bar{\mathbf{S}}[\omega]$, with elements

$$\bar{S}_{ij}[\omega] \times 2\pi\delta[0] = \frac{1}{2} \langle \{ \hat{x}_i[\omega], \hat{x}_j[\omega]^\dagger \} \rangle, \quad (35)$$

where $\{\cdot, \cdot\}$ is the anti-commutator; here, and henceforth, we assume without loss of generality that $\langle \hat{x}_i \rangle = 0$. The SDM is complex-valued, has the symmetry $\bar{\mathbf{S}}[\omega]^* = \bar{\mathbf{S}}[-\omega]$, and it is hermitian positive semi-definite (HPSD), as shown in Theorem 7 of Appendix A.

In the frequency-independent case, the noise properties are encoded in the covariance matrix $\mathbf{V} := \bar{\mathbf{S}}[0]$. It is real-valued, symmetric, and positive semi-definite. In this setting, the uncertainty principle states that [51] $\mathbf{V} + i\mathbf{J}/2$ is hermitian positive semi-definite, i.e.

$$\mathbf{V} + \frac{i}{2}\mathbf{J} \geq 0. \quad (36)$$

In particular, for a single mode, it yields the inequality

$$V_{qq}V_{pp} - V_{qp}^2 \geq \frac{1}{4}. \quad (37)$$

A. Conjugate symplectic uncertainty principle and invariant reduction of SDM

In the frequency-dependent case we can show (see SI Section V) that the uncertainty principle can be stated as follows.

Theorem 3. *Let $\bar{\mathbf{S}}[\omega]$ be the SDM of n weak-stationary quantum noises. For any $\omega \in \mathbb{R}$, the matrix $\bar{\mathbf{S}}[\omega] + i\mathbf{J}/2$ is hermitian, positive semi-definite, i.e.*

$$\bar{\mathbf{S}}[\omega] + \frac{i}{2}\mathbf{J} \geq 0. \quad (38)$$

Despite the superficial similarity to the frequency-dependent case [Eq. (36)], the content of this inequality is subtly different. In particular, since the SDM is hermitian (and not symmetric, like the covariance matrix), even for a single quantum noise $\{\hat{q}(t), \hat{p}(t)\}$, Theorem 3 implies

$$\bar{S}_{qq}[\omega]\bar{S}_{pp}[\omega] - |\bar{S}_{qp}[\omega]|^2 \geq \frac{1}{4} + |\text{Im}(\bar{S}_{qp}[\omega])|, \quad (39)$$

which is tighter compared to the frequency-independent case [Eq. (37)] due to the imaginary cross correlation term.

This qualitatively novel feature turns out to be fundamental in the phenomenology of frequency-dependent quantum LTI systems. In order to characterize the origin and structure of the imaginary cross-correlation, we seek a convenient normal form of the SDM. Since the LTI

transformation $\hat{\mathbf{x}}[\omega] \mapsto \mathbf{M}[\omega]\hat{\mathbf{x}}[\omega]$ induces the transformation on the SDM $\bar{\mathbf{S}}[\omega] \mapsto \mathbf{M}[\omega]\bar{\mathbf{S}}[\omega]\mathbf{M}[\omega]^\dagger$, our interest is limited to a normal form from which every SDM can be generated by an LTI transformation. The following theorem achieves precisely such a characterization (see SI Section VI for proof).

Theorem 4. *Let $\bar{\mathbf{S}}$ be the SDM of an n weak-stationary quantum noises. For any frequency $\omega \in \mathbb{R}$, there exists*

- $\mathbf{M}[\omega] \in \text{Sp}^\dagger(2n)$ such that $\mathbf{M}[-\omega] = \mathbf{M}[\omega]^*$;
- a diagonal matrix $\boldsymbol{\Sigma}[\omega] = \text{diag}(\Sigma_1[\omega], \dots, \Sigma_n[\omega])$ with Σ_j a positive even function for any $j \in \{1, \dots, n\}$;
- a diagonal matrix $\boldsymbol{\Delta}[\omega] = \text{diag}(\Delta_1[\omega], \dots, \Delta_n[\omega])$ with Δ_j an odd function for any $j \in \{1, \dots, n\}$, satisfying

$$\Sigma_j[\omega] \geq \frac{1}{2} + |\Delta_j[\omega]|; \quad (40)$$

such that

$$\bar{\mathbf{S}}[\omega] = \mathbf{M}[\omega] \begin{bmatrix} \boldsymbol{\Sigma}[\omega] & +i\boldsymbol{\Delta}[\omega] \\ -i\boldsymbol{\Delta}[\omega] & \boldsymbol{\Sigma}[\omega] \end{bmatrix} \mathbf{M}[\omega]^\dagger. \quad (41)$$

The elements $\{\boldsymbol{\Sigma}, \boldsymbol{\Delta}\}$ are given by

$$\Sigma_j = \frac{\mu_j - \mu_{n+j}}{2} > 0, \quad \Delta_j = \frac{\mu_j + \mu_{n+j}}{2}, \quad (42)$$

where $\mu_1 \geq \dots \geq \mu_n > 0 > \mu_{n+1} \geq \dots \geq \mu_{2n}$ are the eigenvalues (counting degeneracy) of the matrix $i\mathbf{J}\bar{\mathbf{S}}$ in decreasing order.

This generalizes Williamson's theorem [31] for the real symplectic group. To wit, we know that (setting $\omega = 0$), $\mathbf{M}[0] \in \text{Sp}(2n, \mathbb{R})$, and Theorem 4 asserts that, $\mathbf{V} = \bar{\mathbf{S}}[0] = \mathbf{M} \text{diag}(\boldsymbol{\Sigma}, \boldsymbol{\Sigma}) \mathbf{M}^\dagger$. (Here, $\boldsymbol{\Delta}$ vanished due to its odd symmetry.) That is, any real covariance matrix can be generated by a real symplectic transformation of a diagonal covariance matrix. It can be shown that there exists an n -mode thermal state with average occupation [28, 30, 51] $\langle \hat{n}_j \rangle = \Sigma_j - \frac{1}{2}$. That is, any covariance matrix of an n frequency-independent modes can be prepared by a real symplectic transformation of a suitable set of n thermal states.

Theorem 4 states that the frequency-dependent case is qualitatively different. First, a general SDM results from a conjugate symplectic transformation of the irreducible (non-diagonal) SDM $[\boldsymbol{\Sigma}, +i\boldsymbol{\Delta}; -i\boldsymbol{\Delta}, \boldsymbol{\Sigma}]$. The imaginary off-diagonal term here is precisely the origin of the imaginary cross-correlation in the uncertainty bound in Eq. (39); in fact, Eq. (40) is equivalent to Eq. (39). Thus, complete characterization of the outputs of such systems need to be sensitive to the imaginary cross-correlation $i\boldsymbol{\Delta}$; Section V illustrates such measurement schemes. Second, the pair $\{\boldsymbol{\Sigma}, \boldsymbol{\Delta}\}$ captures the features of the quantum noises that are invariant to conjugate symplectic transformations. That is, the output of a *closed* quantum LTI system will have the same $\{\boldsymbol{\Sigma}, \boldsymbol{\Delta}\}$ as its input. Therefore these features can only arise in the first place from an open quantum LTI system.

B. Nature and origin of the conjugate symplectic invariants

An open system can be modeled starting from a closed system with a conjugate symplectic matrix M^{ext} , explicitly partitioning it into its accessible and inaccessible parts [Eq. (15)] $M^{\text{ext}} = [G, N; K, L]$, then using the generalized Williamson decomposition to write its total output SDM

$$\bar{S}[\omega] = \begin{bmatrix} G & N \\ K & L \end{bmatrix} \begin{bmatrix} \Sigma & +i\Delta \\ -i\Delta & \Sigma \end{bmatrix} \begin{bmatrix} G & N \\ K & L \end{bmatrix}^\dagger, \quad (43)$$

and omitting all but the accessible output (as in Fig. 1(c)). The SDM of this accessible output is the top left corner of the above matrix (independent of K, L ; we also assume for simplicity that the subsystem dimensions are compatible as follows):

$$\bar{S}^{\text{out}} = (G\Sigma G^\dagger + N\Sigma N^\dagger) + i(G\Delta N^\dagger - N\Delta G^\dagger). \quad (44)$$

The first term can be interpreted as noise at the outputs (accessible or inaccessible) of the system transferred from the respective inputs. By contrast, the second term represents the output arising from correlations between the accessible and inaccessible inputs.

The precise interpretation of these matrices can be elucidated by transforming the irreducible SDM in terms of the creation/annihilation operators $\hat{\mathbf{a}}$:

$$\begin{bmatrix} \Sigma[\omega] & +i\Delta[\omega] \\ -i\Delta[\omega] & \Sigma[\omega] \end{bmatrix} \mapsto \begin{bmatrix} \Sigma[\omega] - \Delta[\omega] & \mathbf{0} \\ \mathbf{0} & \Sigma[\omega] + \Delta[\omega] \end{bmatrix}, \quad (45)$$

(see Eq. (A12)) and identifying the latter with the generic SDM in terms of the creation/annihilation operators, whose diagonal elements are $\langle \hat{a}_j[\mp\omega]^\dagger \hat{a}_j[\mp\omega] \rangle + 1 = \langle \hat{n}_j[\mp\omega] \rangle + 1$. This gives, $\langle \hat{n}_j[\pm\omega] \rangle = \Sigma_j[\omega] \pm \Delta_j[\omega] - \frac{1}{2}$, or equivalently

$$\Sigma_j[\omega] = \frac{\langle \hat{n}_j[+\omega] \rangle + \langle \hat{n}_j[-\omega] \rangle}{2} + \frac{1}{2} \quad (46)$$

$$\Delta_j[\omega] = \frac{\langle \hat{n}_j[+\omega] \rangle - \langle \hat{n}_j[-\omega] \rangle}{2} \quad (47)$$

That is, $\Sigma_j[\omega]$ represents the symmetrized thermal occupation, while $\Delta_j[\omega]$ is the sideband asymmetry in the average quantum number.

A concrete scheme to generate sideband asymmetry in the output of an open system can be constructed by employing the optical decomposition of the conjugate symplectic group (Theorem 2). The simplest possibility is a closed system that acts on a pair of quantum noises, followed by elimination of one of its outputs. For example, consider the system depicted in Fig. 3, which is represented by the $\text{Sp}^\dagger(4)$ transfer matrix

$$M = \begin{bmatrix} D & \mathbf{0} \\ \mathbf{0} & D^{-1} \end{bmatrix} \begin{bmatrix} W_2 & \mathbf{0} \\ \mathbf{0} & W_2 \end{bmatrix} \begin{bmatrix} C & -S \\ S & C \end{bmatrix} \begin{bmatrix} W_1 & \mathbf{0} \\ \mathbf{0} & W_1 \end{bmatrix} \quad (48)$$

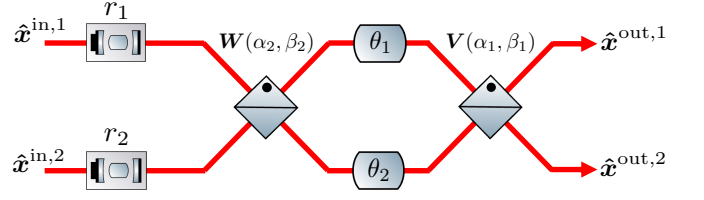


FIG. 3. Two-mode general symplectic transformation acting on vacuum. Appropriately choosing the frequency-dependent coefficients $\alpha_1, \alpha_2, \beta_1, \beta_2, \theta_1$ and θ_2 enables the generation of the $\{\Sigma, \Delta\}$ form of Eq. (49).

where $D = \text{diag}(e^{r_1}, e^{r_2})$, $C = \text{diag}(\cos \theta_1, \cos \theta_2)$, $S = \text{diag}(\sin \theta_1, \sin \theta_2)$, and $W_i = [\cos \alpha_i, -e^{i\beta_i} \sin \alpha_i; e^{-i\beta_i} \sin \alpha_i, \cos \alpha_i]$ with the choice $\alpha_1 = \alpha_2 = \pi/4, \beta_1 = \pi/2, \beta_2 = 0, \theta_1 = \pi/2, \theta_2 = 0$. Let this system be fed with vacuum inputs, i.e. $\bar{S}^{\text{in}} = \mathbf{1}/2$. Then the SDM of one of its outputs (i.e. after eliminating the other) is

$$\bar{S}^{\text{out},2} = \begin{bmatrix} \Sigma & i\Delta \\ -i\Delta & \Sigma \end{bmatrix} \quad (49)$$

where

$$\Sigma = \frac{1}{2} (\cosh^2 r_2 + \cosh^2 r_1) \quad (50)$$

$$\Delta = \frac{1}{2} (\sinh^2 r_2 - \sinh^2 r_1) \quad (51)$$

That is, the outputs of a pair of squeezers, passed through an interferometer, produces in one of its arms, after having eliminated the other, the irreducible SDM that appears in the generalized Williamson decomposition. This scheme can be naturally generalized to generate a n -mode irreducible SDM by starting with a $2n$ -mode vacuum and applying the scheme for the n pairs of modes, then tracing out on half of them.

C. Tighter uncertainty bound for open LTI systems

The uncertainty relations derived above [Eqs. (39) and (40)] apply when the system is closed, and therefore described by a conjugate symplectic transfer matrix. Quite often, as discussed in Section II C, only an open subsystem is accessible. This subsystem is then described by an input-output relation [Eq. (8)]

$$\hat{\mathbf{x}}^{\text{out}}[\omega] = G[\omega]\hat{\mathbf{x}}^{\text{in}}[\omega] + N[\omega]\hat{\mathbf{x}}^{\text{N}}[\omega], \quad (52)$$

where G is usually known, and N is reconstructed from it (see Section II B); neither of them need be conjugate symplectic. The theorem below bounds the uncertainty of the accessible outputs when the inaccessible inputs cannot be quantum engineered, thus yielding a stricter result than the ones derived above for closed systems (see SI Section VII for a proof).

Theorem 5. Assuming that the noise modes (i.e. inaccessible inputs) are uncorrelated with each other and with the input modes, the output modes' spectral densities satisfy, for all $i \in \{1, \dots, n\}$

$$\sqrt{\bar{S}_{q_i q_i}^{\text{out}} \bar{S}_{p_i p_i}^{\text{out}}} \geq \sqrt{\det \sum_{j,k} \mathbf{G}_{ij} \bar{\mathbf{S}}_{jk}^{\text{in}} \mathbf{G}_{ki}^\dagger} + \frac{1}{2} \sum_j |\det \mathbf{N}_{ij}|. \quad (53)$$

where the matrices on the right hand side are defined as: for $\mathbf{A} \in \{\mathbf{G}, \bar{\mathbf{S}}^{\text{in}}, \mathbf{N}\}$,

$$\mathbf{A}_{jk} := \begin{bmatrix} A_{q_j q_k} & A_{q_j p_k} \\ A_{p_j q_k} & A_{p_j p_k} \end{bmatrix}. \quad (54)$$

Note that this inequality is tight when $\bar{S}_{q_i p_i} = 0$, and all of the matrices $\mathbf{N}_{ij} \mathbf{N}_{ji}^\dagger$ are proportional to each other and to $\sum_{j,k} \mathbf{G}_{ij} \bar{\mathbf{S}}_{jk}^{\text{in}} \mathbf{G}_{ki}^\dagger$ (if this term is non-zero). The former is true if, for instance, all of these transfer matrices treat the amplitude and phase quadratures symmetrically. Since the first term on the right-hand-side of Eq. (53) is positive semi-definite, the looser form,

$$\sqrt{\bar{S}_{q_i q_i}^{\text{out}} \bar{S}_{p_i p_i}^{\text{out}}} \geq \frac{1}{2} \sum_j |\det \mathbf{N}_{ij}| \quad (55)$$

also holds, which is still tighter than Theorem 3.

V. SDM TOMOGRAPHY

The central role of the SDM in characterizing the noise performance of quantum LTI systems demands the availability of techniques to experimentally reconstruct it given access to the output ports of a quantum LTI system. Surprisingly, as we will show, conventional homodyne (or heterodyne) measurements of the output noises are not sufficient to reconstruct the SDM. This is a manifestation of the imaginary cross-correlations encoded in the SDM, and its retrieval calls for a modification of the conventional homodyne scheme. We now describe a scheme — called *symplectodyne* measurement — that can overcome the incompleteness inherent in conventional measurements.

A. Single mode case

To illustrate the principle of symplectodyne measurement, we first consider the simple problem of SDM tomography of a single mode. The tomographic reconstruction of its SDM entails the estimation of the elements of the hermitian matrix

$$\bar{\mathbf{S}}[\omega_0] = \begin{bmatrix} \bar{S}_{qq}[\omega_0] & \bar{S}_{qp}[\omega_0] \\ \bar{S}_{qp}[\omega_0]^* & \bar{S}_{pp}[\omega_0] \end{bmatrix}$$

at each frequency ω_0 ; i.e. four real parameters (two diagonal terms, the real and imaginary parts of the cross-correlation) per frequency.

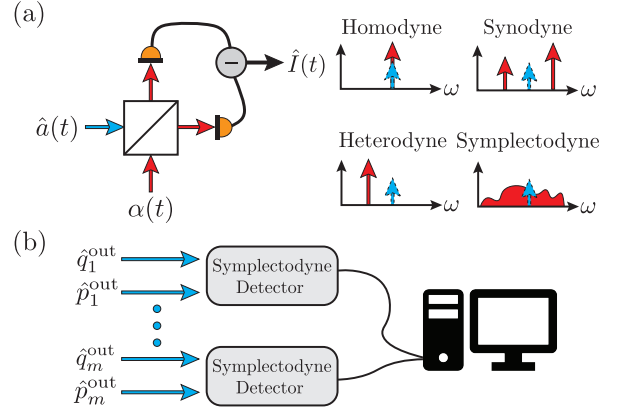


FIG. 4. *Symplectodyne detector.* (a) Shows the implementation of a single-mode symplectodyne detector. The local oscillator $\alpha(t)$ with an arbitrary waveform is coupled to a signal field $\hat{a}(t)$ with a balanced coupler. The spectrum of the differential photocurrent $\hat{I}(t)$ is used to recover the spectral density matrix of the signal. Depending on the local oscillator spectrum, symplectodyne detection subsumes homodyne, heterodyne, or synodyne detection. The relationship between the local oscillator tone (red arrows) and carrier frequency (dashed blue arrows) is indicated for each detection scheme. (b) Multimode SDM tomography can be performed by subjecting the output fields of a quantum LTI system to symplectodyne detection and correlating their output photocurrents.

Consider the scheme shown in Fig. 4(a), wherein a balanced photodetector is fed with the equal superposition of a local oscillator with classical complex-valued amplitude waveform $\alpha(t)$ and the ladder operator $\hat{a}(t)$ of the single-mode “signal” of interest. The linearized photocurrent emitted by the detector is (up to a multiplicative constant, taken to be $1/\sqrt{2}$ for convenience)

$$\hat{I}(t) := \frac{\alpha^*(t)\hat{a}(t) + \alpha(t)\hat{a}^\dagger(t)}{\sqrt{2}} = \boldsymbol{\alpha}(t)^\dagger \hat{\mathbf{x}}(t); \quad (56)$$

here, we have defined the two (real-valued) local oscillator quadratures $\alpha_q(t) = [\alpha(t) + \alpha^*(t)]/2$ and $\alpha_p(t) = i[\alpha(t)^* - \alpha(t)]/2$ arranged into the vector $\boldsymbol{\alpha}(t) = [\alpha_q(t), \alpha_p(t)]^T$. This photocurrent operator is effectively a classical stochastic process if $[\hat{I}(t), \hat{I}(t')] = 0$ for all t, t' [59]; this condition boils down to $J_{ij} \alpha_i(t) \alpha_j(t) = 0$, which is always satisfied on account of the anti-symmetry of \mathbf{J} . Thus, the symplectic matrix plays an essential role, hence the name “symplectodyne” measurement.

The spectrum of the symplectodyne photocurrent is

$$\bar{S}_{II}[\Omega] \times 2\pi\delta[0] = \int_{-\infty}^{+\infty} \frac{d\Omega}{2\pi} \boldsymbol{\alpha}[\Omega]^\dagger \bar{\mathbf{S}}[\omega + \Omega] \boldsymbol{\alpha}[\Omega] \quad (57)$$

Choice of the spectral content of the LO, i.e. the functional form $\boldsymbol{\alpha}[\Omega]$, subsumes the homodyne, heterodyne, or synodyne detection [60] strategies. However, neither homodyne or heterodyne photocurrent spectra contain the full information contained in the SDM of the signal.

To wit, the homodyne case corresponds to the choice $\boldsymbol{\alpha}[\omega] = 2\pi\delta[\omega]|\alpha_0\rangle \times [\cos\theta, \sin\theta]^T$ with $\theta = \arg\alpha_0$. Then Eq. (57) reduces to

$$\bar{S}_{II}^{\text{hom}}[\omega] = \boldsymbol{\alpha}_0^\top \text{Re}(\bar{\mathcal{S}}[\omega]) \boldsymbol{\alpha}_0 \quad (58)$$

where $\boldsymbol{\alpha}_0 = [\text{Re}(\alpha_0), \text{Im}(\alpha_0)]^\top \in \mathbb{R}^2$. Note that the photocurrent is only sensitive to the real part of the off-diagonal elements (\bar{S}_{qp}) of the SDM; i.e. homodyne detection is blind to the imaginary cross-correlations [61, 62], which can hide quantum resources detailed in Section VIB. Heterodyne detection corresponds to the choice $\boldsymbol{\alpha}[\omega] = 2\pi\alpha_0\delta[\omega - \omega_0]$, where $\alpha_0 \in \mathbb{C}$, so that Eq. (57) reduces to

$$\begin{aligned} \bar{S}_{II}^{\text{het}}[\omega] &= \frac{|\alpha_0|^2}{4} [\bar{S}_{qq}[\omega_0 + \omega] + \bar{S}_{qq}[\omega_0 - \omega] \\ &\quad + \bar{S}_{pp}[\omega_0 + \omega] + \bar{S}_{pp}[\omega_0 - \omega] \\ &\quad + 2\text{Im}(\bar{S}_{qp}[\omega_0 + \omega] + \bar{S}_{qp}[\omega_0 - \omega])]. \end{aligned} \quad (59)$$

Contrary to homodyne detection the heterodyne spectrum reveals the quantum noise at both positive and negative offsets around ω_0 , but it is incomplete in the sense that it isn't sensitive to the real part of the cross-correlation.

Complete information in the signal SDM can be captured using a two-tone local oscillator symmetric about the carrier frequency, i.e. the choice $\boldsymbol{\alpha}[\omega] = \sqrt{2\pi}(\alpha_+\delta[\omega - \omega_0] + \alpha_-\delta[\omega + \omega_0])$, where $\alpha_+, \alpha_- \in \mathbb{C}$. This scheme is a form of quadrature amplitude demodulation (see Supplementary Information Section VIII), and has apparently been re-discovered under the guise of ‘‘synodyne’’ detection [60]. With this choice of LO, Eq. (57) at $\omega = 0$ reduces to

$$\bar{S}_{II}[0] = \boldsymbol{\alpha}_0^\dagger \bar{\mathcal{S}}[\omega_0] \boldsymbol{\alpha}_0 =: Q(\alpha_{q0}, \alpha_{p0}), \quad (60)$$

a hermitian form $Q(\cdot, \cdot)$ of the elements of the vector

$$\boldsymbol{\alpha}_0 = \frac{1}{2} \begin{bmatrix} \alpha_+ + \alpha_-^* \\ i(\alpha_-^* - \alpha_+) \end{bmatrix} =: \begin{bmatrix} \alpha_{q0} \\ \alpha_{p0} \end{bmatrix} \in \mathbb{C}^2. \quad (61)$$

The SDM $\bar{\mathcal{S}}[\omega_0]$ can be reconstructed from photocurrent measurements by suitable choices of $\boldsymbol{\alpha}_0$. Indeed, its diagonal entries are given by $\bar{S}_{qq}[\omega_0] = Q(\alpha_{q0}, 0)/|\alpha_{q0}|^2$ and $\bar{S}_{pp}[\omega_0] = Q(0, \alpha_{p0})/|\alpha_{p0}|^2$, while the real and imaginary parts of the cross-correlation are given by (tuning the relative phase between the q and p quadratures of the modulated LO):

$$\text{Re}(\bar{S}_{qp}[\omega_0]) = \frac{Q(\alpha_{q0}, \alpha_{p0}) - Q(\alpha_{q0}, -\alpha_{p0})}{4|\alpha_{q0}|^2}, \quad (62a)$$

$$\text{Im}(\bar{S}_{qp}[\omega_0]) = \frac{Q(\alpha_{q0}, -i\alpha_{p0}) - Q(\alpha_{q0}, i\alpha_{p0})}{4|\alpha_{q0}|^2}. \quad (62b)$$

Note that in practice, it is not necessary to access the photocurrent spectrum at exactly $\omega = 0$; the above expressions remain well-approximated over a bandwidth

of frequencies for which $\bar{\mathcal{S}}[\omega]$ does not vary significantly. That is, if the spectral feature of interest in $\bar{\mathcal{S}}$ is in a bandwidth $\Delta\omega$ around ω_0 , then

$$\bar{S}_{II}[\omega] \underset{\omega \ll \Delta\omega}{\approx} \boldsymbol{\alpha}_0^\dagger \bar{\mathcal{S}}[\omega_0] \boldsymbol{\alpha}_0 \quad (63)$$

confirming that synodyne detection is feasible.

B. Multimode symplectodyne detection

The discussion above can be naturally generalized to n signals described by their quadratures $\hat{\boldsymbol{x}}(t) = [\hat{q}_1(t), \dots, \hat{q}_n(t), \hat{p}_1(t), \dots, \hat{p}_n(t)]^T$, since Eqs. (56) and (57) for the photocurrent and its spectrum stay valid for a n -mode local oscillator $\boldsymbol{\alpha}(t) = [\alpha_{q_1}(t), \dots, \alpha_{q_n}(t), \dots, \alpha_{p_1}(t), \dots, \alpha_{p_n}(t)]^T \in \mathbb{R}^{2n}$. The general photocurrent $\hat{I} = \boldsymbol{\alpha}(t)^\dagger \hat{\boldsymbol{x}}(t)$ can be realized (even without a multimode combiner) by performing synodyne detection on each of the n modes separately, yielding the single-mode photocurrents $\hat{I}_m(t) = \alpha_{q_m}(t)\hat{q}_m(t) + \alpha_{p_m}(t)\hat{p}_m(t)$, which are themselves effectively classical stochastic processes, and therefore capable of being recorded and combined electronically to obtain the desired sum photocurrent $\hat{I}(t)$. This scheme is shown in figure Fig. 4(b).

VI. APPLICATIONS

To illustrate the physical insight of the conjugate symplectic group, we highlight various examples of physical systems on which the previous results apply.

A. Single and two-mode synthesis

In case of a single mode, the conjugate symplectic group reduces to the product of the circle group with the real symplectic group: $\text{Sp}^\dagger(2) = U(1) \times \text{Sp}(2n, \mathbb{R})$ as can be explicitly seen in the optical decomposition theorem [Theorem 2]. This form represents the frequency-dependent rotation of squeezing, as implemented in gravitational-wave detectors [63, 64]. The observable statistical moments are contained in the single mode SDM, which is real-valued. Therefore, for a single mode, the conjugate symplectic formulation is essentially equivalent to a real symplectic treatment for every frequency. This is no longer true for two or more modes.

Indeed, for $n = 2$, each matrix factor that appears in Theorem 2 can be explicitly identified with a two-input/two-output optical component. The salient element is the frequency-dependent beam-splitter, $\text{diag}(\mathbf{U}, \mathbf{U})$ with $\mathbf{U} \in U(2)$, which imprints complex rotations to the two-mode state. (Such a beam-splitter can be realized using a critically-coupled resonator, see Supplementary Information Section IX.) Thus the conjugate symplectic framework is essential and qualitatively distinct from the

real-symplectic formalism, since the cross-correlations between the quadratures of a mode are now complex-valued in general.

B. Complex squeezing: its generation and diagnosis

The inescapable physical manifestation of complex-valued cross-correlations is the phenomenon of “complex” squeezing. This phenomenon, predicted in various quantum systems such as optomechanical devices [60, 65] (including gravitational-wave detectors [25]) and Kerr microresonators [62, 66, 67], is still poorly understood within a systematic framework. In particular, it is unknown what the sufficient requirement to produce complex squeezing is, and how its presence can be diagnosed. Indeed, in gravitational-wave detectors, the precise failure to resolve complex squeezing through homodyne detection — termed “dephasing” [25, 68] — has been considered a fundamental source of squeezing degradation. In the following, we show the sufficient condition to produce complex squeezing, and how it can be uncovered by symplectodyne measurements.

$$\bar{\mathcal{S}}_{\text{out}}[\omega] = \frac{1}{2} \begin{bmatrix} 1 + (F_+^2 + F_-^2) \sinh^2 r + F_- F_+ \cos(2\theta_D) \sinh(2r) & F_+ F_- \sin(2\theta_D) \sinh(2r) + i(F_+^2 - F_-^2) \sinh^2 r \\ F_+ F_- \sin(2\theta_D) \sinh(2r) - i(F_+^2 - F_-^2) \sinh^2 r & 1 + (F_+^2 + F_-^2) \sinh^2 r - F_- F_+ \cos(2\theta_D) \sinh(2r) \end{bmatrix} \quad (64)$$

where $\theta_D[\omega] = \arg(F[\omega]F[-\omega])/2$, and we used the shorthand notation $F_{\pm} := |F[\pm\omega]|$. The complex cross-correlations, described by the off-diagonal term $\pm i(F_+^2 - F_-^2) \sinh^2 r$, become apparent when the losses are asymmetric in frequency ($F_+ \neq F_-$) and increase with the level of input squeezing r .

A physical system that presents such asymmetric-in-frequency loss for input frequency-independent squeezing is a detuned critically-coupled optical cavity. The vacuum mode coupled through the end mirror of the cavity combined with the resonance condition represent the frequency-dependent loss, while the detuning induces the necessary sideband imbalance $F_+ \neq F_-$ for complex squeezing. The magnitude of the cavity response is

$$|F[\omega]|^2 = \frac{4R \sin^2(\phi[\omega])}{(1-R)^2 + 4R \sin^2(\phi[\omega])} \quad (65)$$

where R is the power reflectivity of either mirror of the cavity, $\phi[\omega] = \omega L_0/c + \phi_0$ is the single-trip phase, with L_0 the resonant length of the cavity and $\phi_0 \in [0, 2\pi]$ the detuning of the cavity from the carrier resonance, which can be arbitrarily tuned by the user. Choosing R and ϕ_0 allows to realize any set of values for the sideband efficiencies $(F_+^2, F_-^2) \in [0, 1]^2$.

In order to show that $\bar{\mathcal{S}}_{\text{out}}[\omega]$ displays complex squeezing, we compare the lowest eigenvalues of $\bar{\mathcal{S}}_{\text{out}}[\omega]$ and $\text{Re}(\bar{\mathcal{S}}_{\text{out}}[\omega])$, namely Λ_-^{C} and Λ_-^{R} . As per the discussion in Section V, a symplectodyne (respectively, homodyne)

We define complex (or hidden) squeezing as follows.

Definition 7. (*Complex squeezing*) Given a single-mode SDM $\bar{\mathcal{S}}[\omega]$, we say that the underlying quantum state possesses complex (or hidden) squeezing if the smallest eigenvalue of $\bar{\mathcal{S}}$ is lower than $1/2$, while the smallest eigenvalue of $\text{Re}(\bar{\mathcal{S}})$ is larger than $1/2$.

Since a homodyne detector is only sensitive to $\text{Re}(\bar{\mathcal{S}})$, homodyne detectors are blind to complex squeezing; however, they can be resolved as sub-vacuum fluctuations in a symplectodyne detector.

In order to understand the origin of complex squeezing, consider a frequency-independent squeezed single mode, described by its SDM $\bar{\mathcal{S}}_{\text{in}} = \text{diag}(e^r/2, e^{-r}/2)$, passing through a lossy passive system, as shown in Fig. 5(a). The input-output relation is classically described by the relation $a_{\text{out}}[\omega] = F[\omega] a_{\text{in}}[\omega]$ where $|F[\omega]| \leq 1$. Using the approach described in II C, the quantum description of such a system requires a single additional noise mode. The output SDM is entirely determined by $F[\omega]$ and reads

detector is sensitive to the former (latter). These eigenvalues are shown in Fig. 5(c): as the input squeezing level increases, the homodyne detector is oblivious to the presence of squeezing, whereas a symplectodyne detector resolves it below the vacuum level. Thus the state is complex squeezed. Indeed, it can be shown (see Supplementary Information Section X) that in the limit of high squeezing,

$$\begin{aligned} \Lambda_-^{\text{C}} &\xrightarrow{r \rightarrow \infty} \frac{1}{2} [(1 - \eta^{\text{C}}) + \eta^{\text{C}} e^{-2r}] < \frac{1}{2} \\ \Lambda_-^{\text{R}} &\xrightarrow{r \rightarrow \infty} \frac{1}{8} (F_+ - F_-)^2 e^{2r} \gg \frac{1}{2} \end{aligned} \quad (66)$$

where $\eta^{\text{C}} = 2/(F_-^{-2} + F_+^{-2})$ is the *harmonic mean* of the single sideband efficiencies at $\pm\omega$.

The threshold of input squeezing r_{lim} for which squeezing becomes hidden, obtained by solving for $\Lambda_-^{\text{R}}(r_{\text{lim}}) = 1/2$, yields the simple form

$$r_{\text{lim}} = \text{arctanh} \left(\frac{2F_+ F_-}{F_+^2 + F_-^2} \right) \quad (67)$$

For input squeezing level $r > r_{\text{lim}}$, the squeezing properties present in $\bar{\mathcal{S}}_{\text{out}}$ are completely hidden in the complex correlations, and homodyne detection fails at identifying this quantum resource, see Fig. 5(b). Worse, it identifies the state in question as having increasingly large classical fluctuations (scaling as e^{2r}) even in the optimal

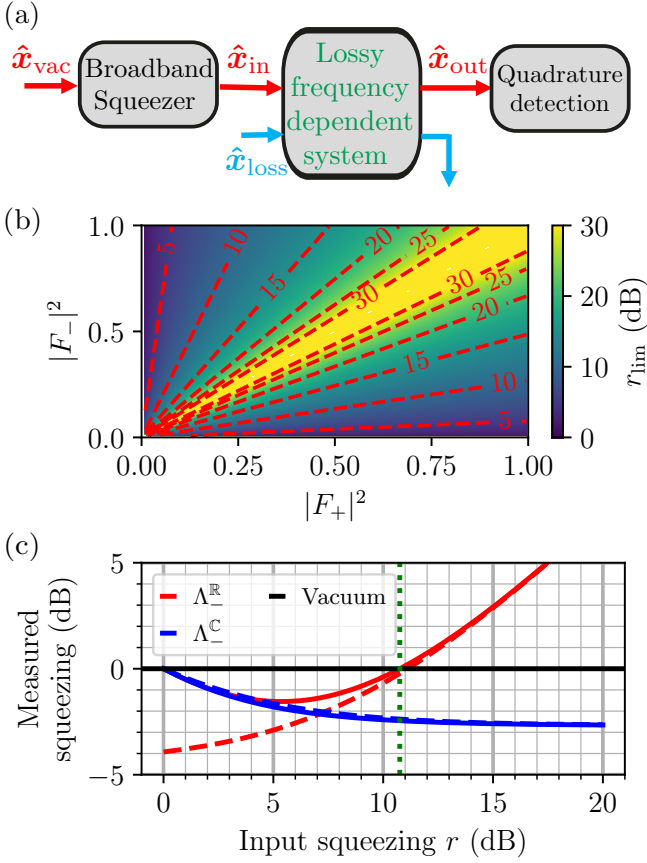


FIG. 5. (a) General scheme for production of complex squeezing, and its detection. (b) Disappearance of squeezing in a homodyne detector due to frequency-dependent loss. The plot shows the limiting value of input squeezing (r_{lim} in Eq. (67)) in dB units at which a homodyne detector fails to diagnose the presence of squeezing due to frequency-dependent losses F_+ and F_- . (c) Comparison of the optimal quadrature measurement for a lossy system described by Eq. (64), using homodyne (Λ_{-}^{R} , red) or syndyne detection (Λ_{-}^{C} , blue). The sideband efficiencies are taken to be $F_+^2 = 0.99$ and $F_-^2 = 0.3$. The dashed lines are the asymptotic expressions in Eq. (66). The green vertical line shows r_{lim} , above which the measured squeezing becomes hidden.

quadrature, whereas a symplectodyne detector accurately diagnoses its quantum nature.

Importantly, the apparent loss of squeezing due to frequency-dependent loss (observed in gravitational-wave detectors [25]) is not a fundamental limit but rather a penalty due to the choice of sub-optimal detection schemes. Similarly, other quantum information schemes which require high levels of optical squeezing [69–71] can have apparent degradation of quantum resources due to dispersive lossy components, unless a proper detection scheme is employed.

The scheme sketched above applies to frequency-dependent *loss*; but similar phenomenology also applies to frequency-dependent *gain*, such as in phase-mixing amplifiers [72], though their minimal description requires

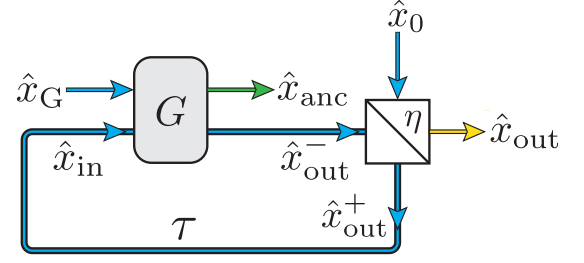


FIG. 6. A quantum feedback oscillator in which the output of an amplifier, labeled G , is partially out-coupled and partially fed back to its input by a beam splitter labeled η after a time delay τ . For most physical feedback oscillators, such as lasers, the quantum noise inputs \hat{x}_0 and \hat{x}_{G} to the beam splitter and amplifier are inaccessible, the amplifier’s output, \hat{x}_{anc} is inaccessible, and the field out-coupled by the beam splitter, \hat{x}_{out} gives the system’s accessible output.

up to two additional noise modes.

C. Tight quantum noise limits for linear feedback oscillators: The Schawlow-Townes limit

The quantum noise performance of a laser, described by the Schawlow-Townes formula, is a fundamental problem in quantum optics. It has been shown [32] that the Schawlow-Townes formula is a general feature of all feedback oscillators, and that it can be evaded by quantum engineering the amplifier and out-coupler in the feedback loop of an oscillator. But the question of whether it is possible to suppress output fluctuations all the way to the minimum level imposed by the Heisenberg uncertainty bound [Eq. (39)] remained open.

In order to settle this question in the affirmative, we revisit the simple model of a feedback oscillator as a two-input, two-output device (see Fig. 6) where the device’s outputs carry quantum fluctuations on top of a mean macroscopic signal as depicted in Fig. 6. The device’s observed output \hat{x}_{out} and unobserved output \hat{x}_{anc} , are related to the noise inputs to the beam splitter, \hat{x}_0 , and amplifier, \hat{x}_{G} , by [32], $[\hat{q}_{\text{out}}, \hat{q}_{\text{anc}}, \hat{p}_{\text{out}}, \hat{p}_{\text{anc}}]^{\text{T}} = \mathbf{M}[\hat{q}_0, \hat{q}_{\text{G}}, \hat{p}_0, \hat{p}_{\text{G}}]^{\text{T}}$ where the transfer matrix

$$\mathbf{M}[\omega] = \begin{bmatrix} H_0[\omega] & H_G[\omega] & 0 & 0 \\ e^{i\omega\tau} H_G[\omega] & H_A[\omega] & 0 & 0 \\ 0 & 0 & H_0[\omega] & -H_G[\omega] \\ 0 & 0 & -e^{i\omega\tau} H_G[\omega] & H_A[\omega] \end{bmatrix} \quad (68)$$

can be expressed in terms of the transfer functions

$$\begin{aligned} H_0[\omega] &= \frac{\sqrt{\eta} + e^{i\omega\tau}/\sqrt{\eta}}{1 + e^{i\omega\tau}} \\ H_G[\omega] &= \frac{1/\sqrt{\eta} - \sqrt{\eta}}{1 + e^{i\omega\tau}} \\ H_A[\omega] &= \frac{1/\sqrt{\eta} + \sqrt{\eta}e^{i\omega\tau}}{1 + e^{i\omega\tau}}, \end{aligned} \quad (69)$$

and η is the beam-splitter's power reflectivity, $G = 1/\sqrt{\eta}$ is the amplifier's amplitude gain, and τ is the round trip time delay. It can be verified that $\mathbf{M}[\omega]\mathbf{J}\mathbf{M}[\omega]^\dagger = \mathbf{J}$.

The conjugate symplectic character of \mathbf{M} immediately implies that \mathbf{M}^{-1} also exists as a conjugate symplectic matrix. The corresponding inverse system can be physically implemented if \mathbf{M}^{-1} is causal. This is indeed the case since

$$\mathbf{M}[\omega]^{-1} = \begin{bmatrix} H_A[\omega] & -H_G[\omega] & 0 & 0 \\ -e^{i\omega\tau}H_G[\omega] & H_0[\omega] & 0 & 0 \\ 0 & 0 & H_A[\omega] & H_G[\omega] \\ 0 & 0 & e^{i\omega\tau}H_G[\omega] & H_0[\omega] \end{bmatrix} \quad (70)$$

involves the same transfer functions as those in $\mathbf{M}[\omega]$, each of which is causal. Then, the protocol to saturate the Heisenberg bound for the feedback oscillator is to act with the causal conjugate symplectic matrix $\mathbf{M}[\omega]^{-1}$ on the vacuum inputs of the amplifier and beam-splitter. The feedback oscillator's output mode will then have the quantum fluctuations of a vacuum state.

On the other hand, if the input noise modes \hat{x}_{in} and \hat{x}_{G} are uncorrelated, we can apply the uncertainty bound of Eq. (55) with $\{\mathbf{N}_{ij}\} = \{\mathbf{N}_{\text{out},0}, \mathbf{N}_{\text{out},\text{G}}\}$ where these matrices can be read off from Eq. (68). We find

$$\begin{aligned} \bar{S}_{qq}^{\text{out}}[\omega]\bar{S}_{pp}^{\text{out}}[\omega] &\geq \frac{1}{4} \left(|\det(\mathbf{N}_{\text{out},0})| + |\det(\mathbf{N}_{\text{out},\text{G}})| \right)^2 \\ &\geq \left(|H_G[\omega]|^2 + \frac{1}{2} \right)^2, \end{aligned} \quad (71)$$

where we have used $|H_0[\omega]|^2 = |H_G[\omega]|^2 + 1$ to simplify the final expression. This bound generalizes the Schawlow-Townes limit in the spectral domain at all frequencies, and exactly recovers it around the carrier frequency when quantum fluctuations are distributed equally between the output quadratures. Notably, since the matrices $\mathbf{N}_{\text{out},0}\mathbf{N}_{\text{out},0}^\dagger$ and $\mathbf{N}_{\text{out},\text{G}}\mathbf{N}_{\text{out},\text{G}}^\dagger$ are linearly dependent, the Minkowski inequality becomes equality and this lower bound is achievable. Indeed, using Eq. (68) and assuming the noise modes are in vacuum states, we see that this uncertainty bound saturated, so this lower bound is tight. We note that this tight lower bound is readily proved using the conjugate-symplectic formalism developed in this paper, yet evaded the previous analysis of ref. [32], which proved a slightly weaker bound.

VII. CONCLUSION

We have developed the first complete theory of quantum linear time-translation-invariant systems, effectively providing a means to arrive at a consistent quantum description of a classical LTI system. In particular, this quantization process proceeds by promoting a classical LTI system to a quantum LTI system with additional quantum noise; we derived the minimal level of added

quantum noise required to enable this transformation. The result is in general an open quantum system. We established a procedure to dilate it into a closed quantum LTI system which evolves unitarily and is described by an element of the conjugate symplectic group $\text{Sp}^\dagger(2n)$.

The conjugate symplectic group is a Lie group, which subsumes the oft-studied real-symplectic group in the realm of Gaussian quantum information theory. We elucidated the structure of the conjugate symplectic group, in particular its one-parameter unitary representation, which gives the Hamiltonian describing these systems. We proved a decomposition theorem that enables synthesis of an arbitrary quantum LTI system in terms of readily constructed optical elements. This synthesis procedure extends and completes the theory of network synthesis of classical LTI systems.

The group structure of quantum LTI systems also naturally gives rise to spectral uncertainty bounds for open and closed systems, which are stricter than the ones usually derived for frequency independent systems.

We established a canonical invariant representation of the spectral density matrices of the outputs of quantum LTI systems. This generalizes Williamson's theorem, and identifies a broader class of symplectic invariants that involves a novel form of complex quantum correlation. These complex correlations manifest as complex squeezing, a quantum resource that has evaded systematic analysis thus far. Complex squeezing is undetectable with standard homodyne or heterodyne detectors and require more general symplectodyne detection to be fully revealed, whose theory we established.

With a full theory of quantum LTI systems in hand, we explored several of its immediate implications. In laser theory, this framework immediately results in tight uncertainty bounds for laser stability that generalize the Schawlow-Townes limit, and shows how lasers may be optimally engineered to evade classical bounds on their performance. Similarly, our theory explains the precise origin and mechanism of "dephasing" loss of squeezing due to frequency-dependent lossy systems such as gravitational wave detectors, and how increased squeezing levels may be recovered with optimal detection schemes.

All of this is done without reference to any internal model of the system and therefore applies directly to the measured response of a quantum system without any need for system identification. That should endow the user of this framework with the power to analyze, synthesize, measure, and generally make sense of complex quantum systems as found in their natural laboratory habitat.

ACKNOWLEDGMENTS

J.D. gratefully acknowledges the support of the EU Horizon 2020 Research and Innovation Program under the Marie Skłodowska-Curie Grant Agreement No. 101003460 (PROBES). H. A. L. gratefully acknowledges the support of the National Science Foundation through the LIGO

operations cooperative agreement PHY18671764464.

Appendix A: Notations and conventions

This appendix details the notations and conventions used throughout this article.

The identity matrix in \mathbb{R}^n is written $\mathbf{1}_n$. For a matrix \mathbf{M} , its transpose is denoted \mathbf{M}^T , element-wise complex conjugate is \mathbf{M}^* , and conjugate transpose is $\mathbf{M}^\dagger = (\mathbf{M}^*)^T$. For a single operator \hat{O} living in a Hilbert space, its adjoint is denoted \hat{O}^\dagger . That is, we distinguish between the different spaces on which quantum operators and matrices act. For matrices, the abbreviation ‘‘HP(S)D’’ stands for hermitian positive (semi) definite.

1. Operators in time and frequency domain

Definition 8 (Fourier transform of an operator). *For any operator in time domain $\hat{A}(t)$, we define its Fourier transform $\hat{A}[\omega]$ as*

$$\hat{A}[\omega] = \int_{-\infty}^{+\infty} \hat{A}(t)e^{i\omega t} dt \quad (\text{A1})$$

or equivalently

$$\hat{A}(t) = \int_{-\infty}^{+\infty} \hat{A}[\omega]e^{-i\omega t} \frac{d\omega}{2\pi}. \quad (\text{A2})$$

We will denote the adjoint of $\hat{A}(t)$ by $\hat{A}^\dagger(t)$ or $\hat{A}(t)^\dagger$; however, we distinguish between $\hat{A}^\dagger[\omega]$ which is the Fourier transform of $\hat{A}^\dagger(t)$, and $\hat{A}[\omega]^\dagger$ which is the adjoint of the Fourier transform of $\hat{A}(t)$. These are related as $\hat{A}^\dagger[\omega] = \hat{A}[-\omega]^\dagger$. For a self-adjoint operator $\hat{X}(t)$, i.e. $\hat{X}(t) = \hat{X}^\dagger(t)$, we further have $\hat{X}^\dagger[\omega] = \hat{X}[-\omega]^\dagger = \hat{X}[\omega]$. These remarks mirror the properties for scalar functions and their Fourier transforms: for any function $f: t \mapsto f(t) \in \mathbb{C}$, we denote the complex conjugate of $f(t)$ by $f(t)^*$ or $f^*(t)$ interchangeably; in frequency domain, however, we have for any $\omega \in \mathbb{R}$ that $f[-\omega]^* = f^*[\omega]$. If $f(t) \in \mathbb{R}$ for any $t \in \mathbb{R}$, then $f^*[\omega] = f[-\omega]^* = f[\omega]$.

The convolution of two scalar functions f and g is

$$\begin{aligned} (f \star g)(t) &:= \int_{-\infty}^{+\infty} f(\tau)g(t-\tau)d\tau \\ &= \int_{-\infty}^{+\infty} f[\omega]g[\omega]e^{-i\omega t} \frac{d\omega}{2\pi}. \end{aligned} \quad (\text{A3})$$

Likewise, if $h(t) := f^*(t)g(t)$ (beware that the complex conjugate is on the time-domain function f), then its Fourier transform is

$$h[\omega] = \int_{-\infty}^{+\infty} f[\Omega]^*g[\omega+\Omega] \frac{d\Omega}{2\pi}. \quad (\text{A4})$$

We also recall the Parseval-Plancherel theorem, which can be extended to well-behaved time-domain operators.

Theorem 6. *Let $\hat{A}(t)$ a time-domain operator and f a well-behaved function. Then,*

$$\int_{-\infty}^{+\infty} f^*(t)\hat{A}(t)dt = \int_{-\infty}^{+\infty} f[\omega]^*\hat{A}[\omega] \frac{d\omega}{2\pi}. \quad (\text{A5})$$

2. Correlation and spectral density matrices

The cross-correlation matrix $\bar{\mathbf{S}}(t)$ for the quadratures of an n -mode system is defined as

$$\bar{\mathbf{S}}_{jk}(t) = \frac{1}{2} \langle \{(\hat{\mathbf{x}}_j(t) - \langle \hat{\mathbf{x}}_j(t) \rangle), (\hat{\mathbf{x}}_k(0) - \langle \hat{\mathbf{x}}_k(0) \rangle)\} \rangle. \quad (\text{A6})$$

Assuming that $\langle \hat{\mathbf{x}}_j(t) \rangle = 0$, which we will assume to be true unless specified otherwise, $\bar{\mathbf{S}}_{jk}(t) = \frac{1}{2} \langle \{ \hat{\mathbf{x}}_j(t), \hat{\mathbf{x}}_k(0) \} \rangle$. For the vacuum state

$$\bar{\mathbf{S}}_{\text{vac}}(t) = \frac{1}{2} \delta(t). \quad (\text{A7})$$

The *spectral density matrix* (SDM), $\bar{\mathbf{S}}[\omega]$, is the element-wise Fourier transform of the cross-correlation matrix in the weak-stationary regime: $\bar{\mathbf{S}}[\omega] = \int_{-\infty}^{+\infty} \bar{\mathbf{S}}(t)e^{i\omega t} dt$. Equivalently,

$$\bar{\mathbf{S}}_{ij}[\omega] \times 2\pi\delta[\omega - \omega'] = \frac{1}{2} \langle \{ \hat{x}_i[\omega], \hat{x}_j[\omega]^\dagger \} \rangle. \quad (\text{A8})$$

The following theorem illustrates important properties of the SDM.

Theorem 7 (Properties of the SDM). *For any frequency $\omega \in \mathbb{R}$, $\bar{\mathbf{S}}[\omega]$ is a complex valued, hermitian positive semi-definite matrix and $\bar{\mathbf{S}}[\omega]^* = \bar{\mathbf{S}}[-\omega]$ (where $(\cdot)^*$ is the element-wise complex conjugate).*

Proof. The hermitian nature of the SDM is due to the hermitian symmetry of the dot product. The equality $\bar{\mathbf{S}}[\omega]^* = \bar{\mathbf{S}}[-\omega]$ can be checked explicitly. Let us show that the SDM is positive semi-definite. Let $\boldsymbol{\alpha} = [\alpha_1, \dots, \alpha_{2N}]^T \in \mathbb{C}^{2N}$ and $\hat{A}[\omega] = \alpha_j^* \hat{x}_j[\omega]$. Then

$$\boldsymbol{\alpha}^\dagger \bar{\mathbf{S}} \boldsymbol{\alpha} = \frac{1}{4\pi\delta[0]} \langle \{ \alpha_j^* \hat{x}_j[\omega], \alpha_k \hat{x}_k[\omega]^\dagger \} \rangle = \bar{S}_{AA}[\omega] \geq 0. \quad (\text{A9})$$

□

So far the results are valid without invoking the commutation relations of Eq. (9) on the quadrature vector. Taking this into account yields the uncertainty principle $\bar{\mathbf{S}}[\omega] + \mathbf{i}\mathbf{J}/2 \geq 0$ of Theorem 3. One can also show that $\bar{\mathbf{S}}[\omega]$ is hermitian positive definite at all frequencies, as detailed in SI Section V.

The utility of the SDM is due to the fact that under an LTI transformation of weak-stationary noises of the form Eq. (19), the associated SDM transforms as

$$\bar{\mathbf{S}}_{\text{out}}[\omega] = \mathbf{M}[\omega] \bar{\mathbf{S}}_{\text{in}}[\omega] \mathbf{M}[\omega]^\dagger. \quad (\text{A10})$$

The SDM can also be expressed in terms of the ladder operators $\hat{\mathbf{a}}[\omega]$ as

$$\bar{S}_{jk}^a[\omega] \times 2\pi\delta[0] := \frac{1}{2} \langle \{\hat{\mathbf{a}}_j[-\omega]^\dagger, \hat{\mathbf{a}}_k[-\omega]\} \rangle. \quad (\text{A11})$$

While $\bar{S}^a[\omega]$ is hermitian, the non-hermiticity of the ladder operators imply that, $\bar{S}^a[-\omega]^* \neq \bar{S}^a[\omega]$, contrary to \bar{S} (see Theorem 7). They are nevertheless related through $\bar{S}[\omega] = \mathbf{P}^* \bar{S}^a[\omega] \mathbf{P}^T = \mathbf{P} \bar{S}^a[-\omega]^* \mathbf{P}^\dagger$, which can be shown by direct computation. Using the commutation relations gives the useful expression

$$\bar{S}_{jk}^a[\omega] = \frac{1}{2\pi\delta[0]} \langle \hat{\mathbf{a}}_j[-\omega]^\dagger \hat{\mathbf{a}}_k[-\omega] \rangle + \frac{(\mathbf{I}_n)_{jk}}{2}. \quad (\text{A12})$$

Appendix B: Input-output description of a classical LTI system

We take the input-output response of a classical system to be defined by a sequence of maps $\{\mathcal{G}^t\}$ whose action $\mathbf{x}^{\text{out}}(t) = \mathcal{G}^t[\mathbf{x}^{\text{in}}]$ is to map the input signal $\mathbf{x}^{\text{in}} = \{x_i^{\text{in}}\}$ (at all times) to the output signal value $\mathbf{x}^{\text{out}}(t)$ at the instant t . Thus the system is equivalent to the set $\{\mathcal{G}^t\}$ of multi-input multi-output maps.

Lemma 1. *A multi-input, multi-output, linear map $\mathcal{G}^t = \{\mathcal{G}_i^t\}$, which maps a collection of inputs to a collection of outputs can be decomposed as a collection of linear maps from a single input to a single output.*

Proof. For a system with m outputs, the input-output relation $\mathbf{x}^{\text{out}}(t) = \mathcal{G}^t[\mathbf{x}^{\text{in}}]$ represents a collection of m equations, the i^{th} of which is $x_i^{\text{out}}(t) = \mathcal{G}_i^t[\mathbf{x}^{\text{in}}]$, where \mathcal{G}_i^t is the map from the collection of inputs to the i^{th} output. Let \mathbf{e}_j be the vector with 1 in the j^{th} position and zero elsewhere; so, $\mathbf{x}^{\text{in}} = \sum_j x_j^{\text{in}} \mathbf{e}_j$. Then by linearity

$$\begin{aligned} x_i^{\text{out}}(t) &= \mathcal{G}_i^t \left[\sum_j x_j^{\text{in}} \mathbf{e}_j \right] \\ &= \sum_j \mathcal{G}_i^t [x_j^{\text{in}} \mathbf{e}_j] =: \sum_j \mathcal{G}_{ij}^t [x_j^{\text{in}}]. \end{aligned} \quad (\text{B1})$$

Thus the i^{th} output is a linear superposition of each of the j inputs via the map \mathcal{G}_{ij}^t . The fact that \mathcal{G}_{ij}^t is linear follows by setting all inputs to zero except the j^{th} in Eq. (2). \square

Thus a linear system is represented by a set of single-input single-output linear maps $\{\mathcal{G}_{ij}^t\}$. If we assume that the input signals form a Hilbert space, then the Riesz representation theorem shows that each of the maps can be uniquely represented by a vector in the dual of the Hilbert space.

Theorem 8 (Riesz [73]). *In a Hilbert space \mathcal{H} equipped with the inner product $\langle \cdot, \cdot \rangle$, every linear map \mathcal{G} on it is uniquely represented as $\mathcal{G}[x] = \langle G, x \rangle$.*

Proof. Note first that by the linearity of \mathcal{G} :

$$\mathcal{G}[\mathcal{G}[x]y - x\mathcal{G}[y]] = \mathcal{G}[x]\mathcal{G}[y] - \mathcal{G}[x]\mathcal{G}[y] = 0; \quad (\text{B2})$$

so $\mathcal{G}[x]y - x\mathcal{G}[y] \in \ker \mathcal{G}$, the kernel space of \mathcal{G} . Now choose $y \in (\ker \mathcal{G})^\perp$ such that $\langle y, y \rangle = 1$; then

$$\begin{aligned} \mathcal{G}[x] &= \mathcal{G}[x]\langle y, y \rangle \\ &= \langle y, \mathcal{G}[x]y \rangle \\ &= \langle y, \mathcal{G}[x]y - x\mathcal{G}[y] \rangle + \langle y, x\mathcal{G}[y] \rangle. \end{aligned} \quad (\text{B3})$$

The first term is zero since y and $\mathcal{G}[x]y - x\mathcal{G}[y]$ lie in orthogonal spaces. Thus

$$\mathcal{G}[x] = \langle y, x\mathcal{G}[y] \rangle = \langle \mathcal{G}[y]^* y, x \rangle =: \langle G, x \rangle. \quad (\text{B4})$$

For uniqueness, suppose $\mathcal{G}[x] = \langle G, x \rangle = \langle G', x \rangle$, then $\langle G - G', x \rangle = 0 \forall x$, so $G - G' = 0$ and G is unique. \square

Using Lemma 1, we can extend Theorem 8 to a multi-input, multi-output maps. To wit, using Eqs. (B1) and (B4), we have

$$x_i^{\text{out}}(t) = \sum_j \mathcal{G}_{ij}^t [x_j^{\text{in}}] = \sum_j \langle G_{ij}^t, x_j^{\text{in}} \rangle. \quad (\text{B5})$$

Thus, the set of maps $\{\mathcal{G}^t\}$ is equivalent to the set of matrices $\{\mathbf{G}^t\}$ for a linear system.

For the rest of this section, whenever matrices and vectors are involved, we use the summation convention for indices.

For real-valued signals of finite energy, the natural Hilbert space is $\mathcal{H} = L^2(\mathbb{R})$, for which the inner product is $\langle y, x \rangle = \int y(t)x(t)dt$. In this case Eq. (B5) becomes

$$\begin{aligned} x_i^{\text{out}}(t) &= \mathcal{G}_{ij}^t [x_j^{\text{in}}] = \langle G_{ij}^t, x_j^{\text{in}} \rangle \\ &= \int G_{ij}^t(t') x_j^{\text{in}}(t') dt' =: \int G_{ij}(t, t') x_j^{\text{in}}(t') dt'. \end{aligned} \quad (\text{B6})$$

That is, the set of linear maps $\{\mathcal{G}^t\}$ is equivalent to a set of matrices $\{\mathbf{G}(t, t')\}$ for each pair of instances t, t' .

Next we show that a linear time-translation-invariant (LTI) system's matrices $\{\mathbf{G}(t, t')\}$ are only functions of the time difference $t - t'$, in which case the integral input-output relation in Eq. (B6) becomes a convolution. Recall the definition of a LTI system in Definition 2.

Theorem 9. *The input-output matrices $\{\mathbf{G}(t, t')\}$ of a LTI system assume the form $\mathbf{G}(t, t') = \mathbf{G}(t - t')$, so the input-output response [Eq. (B6)] reduces to a convolution*

$$x_i^{\text{out}}(t) = \mathcal{G}_{ij}^t [x_j^{\text{in}}] = \int G_{ij}(t - t') x_j^{\text{in}}(t') dt'. \quad (\text{B7})$$

Proof. By the definition of time-translation invariance: $\mathcal{G}_{ij}^t [\mathcal{T}^s [x_j^{\text{in}}(t')]] = \mathcal{T}^s [\mathcal{G}_{ij}^t [x_j^{\text{in}}(t')]]$, so

$$\int G_{ij}(t, t' + s) x_j^{\text{in}}(t') dt' = \int G_{ij}(t - s, t') x_j^{\text{in}}(t') dt' \quad (\text{B8})$$

for all $x_j^{\text{in}}(t')$, which implies $G_{ij}(t, t' + s) = G_{ij}(t - s, t')$. Thus, $G_{ij}(t, s) = G_{ij}(t, 0 + s) = G_{ij}(t - s, 0) =: G_{ij}(t - s)$. \square

A LTI system's input-output relation is naturally written in the time domain as a convolution as in Eq. (B7). Taking the Fourier transform of Eq. (B7), we have

$$\mathbf{x}^{\text{out}}[\omega] = \mathbf{G}[\omega]\mathbf{x}^{\text{in}}[\omega]. \quad (\text{B9})$$

Thus any classical LTI system has outputs linearly related to its inputs in the frequency domain, where the relation between inputs and outputs is governed by the frequency-dependent transfer function matrix $\mathbf{G}[\omega]$.

Appendix C: Algorithms for the optical decomposition

The algorithms below implement the optical decomposition at any arbitrary frequency. They are written in pseudo code but use the NumPy indexing and slicing conventions.

- Algorithm 1, SORTEIGENELEMENTS, sorts the eigenelements of an input matrix in $\text{HPD} \cap \text{Sp}^\dagger(2n)$. We assume that the function $\text{DIAGONALIZE}(\mathbf{M})$ returns an unordered list $\boldsymbol{\lambda}$ of eigenvalues (with multiplicities) and the corresponding unitary matrix \mathbf{V} with eigenvectors as columns. It sorts the eigenelements to be compatible with the ordering $\mathbf{M} = \mathbf{V}_0 \begin{bmatrix} \text{diag}(\boldsymbol{\ell}) & \mathbf{0} \\ \mathbf{0} & \text{diag}(\boldsymbol{\ell})^{-1} \end{bmatrix} \mathbf{V}_0^\dagger$ where $\mathbf{V}_0 \in U(2n)$ and $\boldsymbol{\ell} \in (\mathbb{R}_+^*)^n$ ordered in increasing order as $1 \leq \ell_1 \leq \dots \leq \ell_n$ (see ref. [74] page 136).
- Algorithm 2, CSDSP, performs the conjugate symplectic CSD of an input matrix which is conjugate symplectic and unitary (see SI Theorem 8).
- Algorithm 3, SYMPLECTICSPECTRAL, performs the spectral decomposition in $\text{HPD} \cap \text{Sp}^\dagger(2n)$ (see SI Theorem 7, and ref. [74] page 136)
- Algorithm 4, SVDSP, does the Bloch-Messiah decomposition in $\text{Sp}^\dagger(2n)$ (see SI Theorem 7, ref. [74] page 136, and ref. [22]). $\text{POLAR}(\mathbf{M})$ returns the unique right-polar decomposition of an invertible matrix \mathbf{M} .

Algorithm 1 SORTEIGENELEMENTS

```

1: Input
2:    $\mathbf{M} \in \text{Sp}^\dagger(2n)$  hermitian positive definite
3: Output
4:    $(\boldsymbol{\ell}, \boldsymbol{\ell}^{-1}), \mathbf{V}_0$ 
5: procedure SORTEIGENELEMENTS( $\mathbf{M}$ )
6:    $\boldsymbol{\lambda}, \mathbf{V} := \text{DIAGONALIZE}(\mathbf{M})$ 
7:    $n := \text{LEN}(\boldsymbol{\lambda})/2$ 
8:    $\text{order} := \text{ARGSORT}(\boldsymbol{\lambda})$ 
9:    $\text{order} := \text{CONCATENATE}(\text{order}[n : 2n], \text{order}[n - 1 :: -1])$ 
10:    $\triangleright$  We use python indexing here,  $\boldsymbol{\lambda} = (\boldsymbol{\ell}, \boldsymbol{\ell}^{-1})$ .
11:   return  $\boldsymbol{\lambda}[\text{order}], \mathbf{V}[:, \text{order}]$ .
12: end procedure

```

Algorithm 2 CSDSP

```

1: Input
2:    $\mathbf{U} \in \text{Sp}^\dagger(2n) \cap U(2n)$ 
3: Output
4:    $\mathbf{V}, \mathbf{W}, \boldsymbol{\theta}$  as defined in SI Theorem 8
5: procedure CSDSP( $\mathbf{U}$ )
6:    $n = \text{LEN}(\mathbf{U})/2$ 
7:    $\mathbf{U}' := \mathbf{P}^\dagger \mathbf{U} \mathbf{P} \quad \triangleright \mathbf{U}' \in U(n, n) \cap U(2n)$ 
8:    $\mathbf{Q}_1 := \mathbf{U}'[:, n : n]$ 
9:    $\mathbf{Q}_2 := \mathbf{U}'[n :, n :]$   $\triangleright$  SI Eq. (III.40)
10:   $\mathbf{W}^\dagger, e^{2i\boldsymbol{\theta}} := \text{DIAGONALIZE}(\mathbf{Q}_2^\dagger \mathbf{Q}_1)$   $\triangleright$  SI Eq. (III.41)
11:   $\boldsymbol{\theta} := \text{ANGLE}(e^{2i\boldsymbol{\theta}})/2$ 
12:  return  $\mathbf{Q} \mathbf{W}^\dagger e^{-i\boldsymbol{\theta}}, \mathbf{W}, \boldsymbol{\theta}$ 
13: end procedure

```

Algorithm 3 SYMPLECTICSPECTRAL

```

1: Input
2:    $\mathbf{M} \in \text{Sp}^\dagger(2n)$  hermitian positive definite
3: Output
4:    $(\tilde{\mathbf{D}}, \tilde{\mathbf{D}}^{-1}), \mathbf{U}$  as defined in SI Eq. (III.21)
5: procedure SYMPLECTICSPECTRAL( $\mathbf{M}$ )
6:    $\boldsymbol{\lambda}, \mathbf{V} := \text{SORTEIGENELEMENTS}(\mathbf{M})$ 
7:    $n := \text{LEN}(\boldsymbol{\lambda})/2$ 
8:    $\mathbf{V}_1 := \text{ZEROS\_LIKE}(\mathbf{V})$ 
9:    $m' = 0 \quad \triangleright$  Half multiplicity of the eigenvalue 1
10:  for  $j \in \text{RANGE}(n)$  do
11:    if  $\boldsymbol{\lambda}[j] = 1$  then  $\triangleright$  SI Eq. (III.2)
12:       $\mathbf{V}_1[:, j] := \mathbf{V}[:, j]$ 
13:       $\mathbf{V}_1[:, n + j] := -\mathbf{J} \mathbf{V}[:, j]$ 
14:    else
15:       $\mathbf{V}_1[:, j] := \mathbf{V}[:, j]$ 
16:       $\mathbf{V}_1[:, n + j] := \mathbf{V}[:, n + j]$ 
17:       $m' := m' + 1$ 
18:    end if
19:  end for  $\triangleright$  SI Eq. (III.25)
20:   $\tilde{\mathbf{V}} := \mathbf{V}_1[:, \text{CONCATENATE}(\text{RANGE}(m'), \text{RANGE}(n, n + m'))]$   $\triangleright$  Prepare for SI Eq. (III.26)
21:   $\mathbf{J}' := \tilde{\mathbf{V}}^\dagger \mathbf{J} \tilde{\mathbf{V}} \quad \triangleright 2m' \times 2m'$  matrix
22:   $\boldsymbol{\lambda}', \mathbf{V}' := \text{DIAGONALIZE}(\mathbf{J}')$   $\triangleright$  SI Eq. (III.30)
23:   $\boldsymbol{\lambda}' = \boldsymbol{\lambda}'[\text{ARGSORT}(-\boldsymbol{\lambda}')] \quad \triangleright \boldsymbol{\lambda}' \simeq \mathbf{I}_{m'}$ 
24:   $\mathbf{V}' = \mathbf{V}'[\text{ARGSORT}(-\boldsymbol{\lambda}')]
25:   $\mathbf{W}' := \mathbf{V}' \mathbf{P}^\dagger$ 
26:   $\mathbf{W} := \text{BLOCK\_DIAG}([\mathbf{W}', \mathbf{1}_{2n-2m'}])$ 
27:   $\text{perm\_list} = \text{CONCATENATE}(\text{RANGE}(m'), \text{RANGE}(2m', n + m'), \text{RANGE}(n + m', n + 2m'), \text{RANGE}(n + 2m', 2n)) \triangleright \mathbf{Q}^\dagger$ 
  SI Eq. (III.28)
28:   $\mathbf{W} := \mathbf{W}[:, \text{perm\_list}] \quad \triangleright \mathbf{W} \mathbf{Q}^\dagger$ 
29:   $\mathbf{W} := \mathbf{W}[\text{perm\_list}, :] \quad \triangleright \mathbf{Q} \mathbf{W} \mathbf{Q}^\dagger$ 
30:   $\mathbf{U} := \mathbf{V}_1 \mathbf{W}$ 
31:  return  $\boldsymbol{\lambda}, \mathbf{U} \quad \triangleright$  SI Theorem 7 ( $\boldsymbol{\lambda} = (\tilde{\mathbf{D}}, \tilde{\mathbf{D}}^{-1})$ )
32: end procedure$ 
```

Algorithm 4 SVDSP

```

1: Input
2:    $M \in \text{Sp}^\dagger(2n)$ 
3: Output
4:    $U, V, (\tilde{D}, \tilde{D}^{-1})$  as defined in SI Theorem 6
5: procedure SVDSP( $M$ )
6:    $H, U := \text{POLAR}(M)$   $\triangleright M = UH$ 
7:    $\lambda, V := \text{SYMPLECTICSPECTRAL}(H)$   $\triangleright$ 
    $H = V \text{diag}(\lambda) V^\dagger$ 
8:   return  $UV, V^\dagger, \lambda$   $\triangleright M = UV \text{diag}(\lambda) V^\dagger$ 
9: end procedure

```

- [1] L. Zadeh and C. A. Desoer, *Linear System Theory* (McGraw-Hill, 1963).
- [2] R. W. Brockett, *Finite Dimensional Linear Systems* (John Wiley, 1970).
- [3] T. Kailath, *Linear Systems* (Prentice-Hall, 1980).
- [4] W. Cauer, *Synthesis of Linear Communication Networks* (McGraw-Hill, 1958).
- [5] V. Belevitch, *Classical network theory* (Holden-Day, 1968).
- [6] D. C. Youla, *Theory and Synthesis of Linear Passive Time-Invariant Networks* (Cambridge University Press, 2015).
- [7] R. L. Hudson and K. R. Parthasarathy, Quantum Ito's Formula and Stochastic Evolutions, *Communications in Mathematical Physics* **93**, 301 (1984).
- [8] C. Gardiner and M. Collett, Input and output in damped quantum systems: Quantum stochastic differential equations and the master equation, *Physical Review A* **31**, 3761 (1985).
- [9] K. R. Parthasarathy, *An Introduction to Quantum Stochastic Calculus* (Birkhauser, 1992).
- [10] C. W. Gardiner and P. Zoller, *Quantum Noise* (Springer, 1999).
- [11] C. W. Gardiner, Driving a quantum system with the output field from another driven quantum system, *Physical Review Letters* **70**, 2269 (1993).
- [12] J. E. Gough, R. Gohm, and M. Yanagisawa, Linear quantum feedback networks, *Physical Review A* **78**, 062104 (2008).
- [13] M. James, H. Nurdin, and I. Petersen, H-infinity control of Linear Quantum Stochastic Systems, *IEEE Transactions on Automatic Control* **53**, 1787 (2008).
- [14] J. Gough and M. James, The Series Product and Its Application to Quantum Feedforward and Feedback Networks, *IEEE Transactions on Automatic Control* **54**, 2530 (2009).
- [15] A. A. Clerk, M. H. Devoret, S. M. Girvin, F. Marquardt, and R. J. Schoelkopf, Introduction to quantum noise, measurement, and amplification, *Rev. Mod. Phys.* **82**, 1155 (2010).
- [16] A. J. Shaiju and I. R. Petersen, A frequency domain condition for the physical realizability of linear quantum systems, *IEEE Transactions on Automatic Control* **57**, 2033 (2012).
- [17] N. Yamamoto, Coherent versus Measurement Feedback: Linear Systems Theory for Quantum Information, *Physical Review X* **4**, 041029 (2014).
- [18] N. Yamamoto, Decoherence-Free Linear Quantum Subsystems, *IEEE Transactions on Automatic Control* **59**, 1845 (2014).
- [19] J. Combes, J. Kerckhoff, and M. Sarovar, The SLH framework for modeling quantum input-output networks, *Advances in Physics: X* **2**, 784 (2017).
- [20] G. Zhang, S. Grivopoulos, I. R. Petersen, and J. E. Gough, The Kalman Decomposition for Linear Quantum Systems, *IEEE Transactions on Automatic Control* **63**, 331 (2018).
- [21] H. I. Nurdin and N. Yamamoto, *Linear Dynamical Quantum Systems* (Springer, 2017).
- [22] E. Gouzien, S. Tanzilli, V. D'Auria, and G. Patera, Morphing supermodes: A full characterization for enabling multimode quantum optics, *Phys. Rev. Lett.* **125**, 103601 (2020).
- [23] J. Bentley, H. Nurdin, Y. Chen, and H. Miao, Direct approach to realizing quantum filters for high-precision measurements, *Physical Review A* **103**, 013707 (2021).
- [24] J. Bentley, H. Nurdin, Y. Chen, X. Li, and H. Miao, Designing Optimal Linear Detectors: A Bottom-Up Approach, *Physical Review Applied* **19**, 034009 (2023).
- [25] L. McCuller, S. E. Dwyer, A. C. Green, H. Yu, K. Kuns, *et al.*, LIGO's quantum response to squeezed states, *Phys. Rev. D* **104**, 062006 (2021).
- [26] Arvind, B. Dutta, N. Mukunda, and R. Simon, The real symplectic groups in quantum mechanics and optics, *Pramana* **45**, 471 (1995).
- [27] S. L. Braunstein and P. van Loock, Quantum information with continuous variables, *Rev. Mod. Phys.* **77**, 513 (2005).
- [28] C. Weedbrook, S. Pirandola, R. García-Patrón, N. J. Cerf, T. C. Ralph, J. H. Shapiro, and S. Lloyd, Gaussian quantum information, *Reviews of Modern Physics* **84**, 621 (2012).
- [29] C. Fabre and N. Treps, Modes and states in quantum optics, *Reviews of Modern Physics* **92**, 035005 (2020).
- [30] A. Serafini, *Quantum Continuous Variables: A Primer of Theoretical Methods* (CRC Press, 2023).
- [31] J. Williamson, On the algebraic problem concerning the normal forms of linear dynamical systems, *American Journal of Mathematics* **58**, 141 (1936).
- [32] H. A. Loughlin and V. Sudhir, Quantum noise and its evasion in feedback oscillators, *Nature Communications* **14**, 7083 (2023).
- [33] K. J. Blow, R. Loudon, S. J. D. Phoenix, and T. J. Shep-

- herd, Continuum fields in quantum optics, *Phys. Rev. A* **42**, 4102 (1990).
- [34] B. Yurke and J. S. Denker, Quantum network theory, *Physical Review A* **29**, 1419 (1984).
- [35] A. Blais, A. L. Grimsmo, S. M. Girvin, and A. Wallraff, Circuit quantum electrodynamics, *Rev. Mod. Phys.* **93**, 025005 (2021).
- [36] A. C. Silva, *Lectures on Symplectic Geometry*, edited by J.-M. Morel, F. Takens, and B. Teissier (Springer, 2008).
- [37] In Supplementary Information Section II, we prove that a quantum LTI system with n input modes, m output modes and k noise modes can be considered to be a subsystem of a dilated unitary system with $n + k - m$ ancillary output modes. The dilated system will have the same mean dynamics of the map from the n observed inputs to the m observed outputs. Ref. [36] proves a stronger dilation theorem for real-symplectic systems: a Gaussian bosonic channel from n inputs to n outputs can be dilated to a unitary map by adding $2n$ additional modes, such that both the system's mean response and its output noise is preserved in the dilated system. We leave the proof of the full Gaussian bosonic channel dilation theorem to future work. However, we conjecture that a LTI Gaussian bosonic channel from n inputs to n outputs can be dilated to a unitary map by adding $4n$ additional modes. We anticipate that the additional factor of 2 compared to the frequency-independent case comes from lifting the anti-symmetry condition, as in Section II B.
- [38] The conjugate symplectic group $\text{Sp}^\dagger(2n)$ is not to be confused with the complex symplectic group $\text{Sp}(2n, \mathbb{C}) = \{M \in \mathcal{M}_{2n}(\mathbb{C}) \mid MJM^T = J\}$; see remark 2.7 of [45] and references therein.
- [39] We distinguish a transformation $M[\omega]$ which is reversible, i.e. for which a matrix inverse $M^{-1}[\omega]$ exists from a mathematical standpoint only, from a transformation which is *causally* reversible, i.e. for which $M^{-1}[\omega]$ exists and respects causality.
- [40] Note that here we follow the mathematician's convention for defining a generator, which defers from the physicist's convention by an i .
- [41] An equivalent characterization is obtained by the (bijective) transformation $\mathbf{A} \rightarrow \mathbf{J}\mathbf{A}$, in which case, $\text{sp}^\dagger(2n) := \{\mathbf{J}\mathbf{A} \in \mathcal{M}_{2n}(\mathbb{C}) \mid \mathbf{A} \text{ is hermitian}\}$, and $e^{\tau\mathbf{J}\mathbf{A}} \in \text{Sp}^\dagger(2n)$.
- [42] The argument so far has tacitly assumed that any group element can be represented in the form $e^{\tau\mathbf{A}}$; this is true since the exponential map is surjective in $\text{Sp}^\dagger(2n)$ [75, 76]. We have also not been careful about the fact that in the Hilbert space of quantum states, the unitary representation is up to a phase (i.e. a projective unitary representation); however, this phase is irrelevant in any observable.
- [43] C. Bloch and A. Messiah, The canonical form of an antisymmetric tensor and its application to the theory of superconductivity, *Nuclear Physics* **39**, 95 (1962).
- [44] H. Xu, An svd-like matrix decomposition and its applications, *Linear Algebra and its Applications* **368**, 1 (2003).
- [45] A. Edelman and S. Jeong, Fifty three matrix factorizations: A systematic approach (2022), [arXiv:2104.08669 \[math.NA\]](https://arxiv.org/abs/2104.08669).
- [46] A. Knapp, *Lie Groups: Beyond an Introduction*, 2nd ed. (Birkhauser, 2002).
- [47] M. Reck, A. Zeilinger, H. J. Bernstein, and P. Bertani, Experimental realization of any discrete unitary operator, *Phys. Rev. Lett.* **73**, 58 (1994).
- [48] W. R. Clements, P. C. Humphreys, B. J. Metcalf, W. S. Kolthammer, and I. A. Walmsley, Optimal design for universal multiport interferometers, *Optica* **3**, 1460 (2016).
- [49] R. Balian, C. de Dominicis, and C. Itzykson, Forme canonique des transformations de bogoliubov pour les bosons et des transformations (pseudo) orthogonales, *Nuclear Physics* **67**, 609 (1965).
- [50] B. Yurke, Back-action evasion as an alternative to impedance matching, *Science* **252**, 528 (1991).
- [51] R. Simon, N. Mukunda, and B. Dutta, Quantum-noise matrix for multimode systems: U(n) invariance, squeezing, and normal forms, *Physical Review A* **49**, 1567 (1994).
- [52] A. Roy and M. Devoret, Introduction to parametric amplification of quantum signals with Josephson circuits, *Comptes Rendus Physique* **17**, 740 (2016).
- [53] C. M. Caves and B. L. Schumaker, New formalism for two-photon quantum optics. i. quadrature phases and squeezed states, *Phys. Rev. A* **31**, 3068 (1985).
- [54] B. L. Schumaker and C. M. Caves, New formalism for two-photon quantum optics. ii. mathematical foundation and compact notation, *Phys. Rev. A* **31**, 3093 (1985).
- [55] S. L. Danilishin and F. Y. Khalili, Quantum Measurement Theory in Gravitational-Wave Detectors, *Living Reviews in Relativity* **15**, 5 (2012).
- [56] D. Branford, H. Miao, and A. Datta, Fundamental quantum limits of multicarrier optomechanical sensors, *Phys. Rev. Lett.* **121**, 110505 (2018).
- [57] T. Gefen, R. Tarafder, R. X. Adhikari, and Y. Chen, Quantum precision limits of displacement noise-free interferometers, *Phys. Rev. Lett.* **132**, 020801 (2024).
- [58] J. W. Gardner, T. Gefen, S. A. Haine, J. J. Hope, and Y. Chen, Achieving the fundamental quantum limit of linear waveform estimation, *Physical Review Letters* **132** (2024).
- [59] V. P. Belavkin, Nondemolition principle of quantum measurement theory, *Foundations of Physics* **24**, 685 (1994).
- [60] L. Buchmann, S. Schreppler, J. Kohler, N. Spethmann, and D. Stamper-Kurn, Complex Squeezing and Force Measurement Beyond the Standard Quantum Limit, *Physical Review Letters* **117**, 030801 (2016).
- [61] F. A. S. Barbosa, A. S. Coelho, K. N. Cassemiro, P. Nussenzveig, C. Fabre, A. S. Villar, and M. Martinelli, Quantum state reconstruction of spectral field modes: Homodyne and resonator detection schemes, *Phys. Rev. A* **88**, 052113 (2013).
- [62] E. Gouzien, L. Labonté, J. Etesse, A. Zavatta, S. Tanzilli, V. D'Auria, and G. Patera, Hidden and detectable squeezing from microresonators, *Phys. Rev. Res.* **5**, 023178 (2023).
- [63] D. Ganapathy, W. Jia, M. Nakano, V. Xu, N. Aritomi, T. Cullen, N. Kijbunchoo, S. Dwyer, A. Mullavey, L. McCuller, and LIGO O4 Detector Collaboration, Broadband Quantum Enhancement of the LIGO Detectors with Frequency-Dependent Squeezing, *Physical Review X* **13**, 041021 (2023).
- [64] W. Jia, V. Xu, K. Kuns, M. Nakano, L. Barsotti, M. Evans, N. Mavalvala, and members of the LIGO Scientific Collaboration, Squeezing the quantum noise of a gravitational-wave detector below the standard quantum limit, *Science* **385**, 1318 (2024).
- [65] C. Ockeloen-Korppi, E. Damskagg, G. Paroanu, F. Massel, and M. Sillanpää, Revealing hidden quantum correlations in an electromechanical measurement, *Physical Review Letters* **121** (2018).

- [66] M. A. Guidry, D. M. Lukin, K. Y. Yang, and J. Vučković, Multimode squeezing in soliton crystal microcombs, *Optica* **10**, 694 (2023).
- [67] B. Dioum, V. D’Auria, A. Zavatta, O. Pfister, and G. Patena, Universal quantum frequency comb measurements by spectral mode-matching (2024), [arXiv:2405.18454](https://arxiv.org/abs/2405.18454) [quant-ph].
- [68] P. Kwee, J. Miller, T. Isogai, L. Barsotti, and M. Evans, Decoherence and degradation of squeezed states in quantum filter cavities, *Phys. Rev. D* **90**, 062006 (2014).
- [69] S. L. Braunstein and H. J. Kimble, Dense coding for continuous variables, *Physical Review A* **61**, 042302 (2000).
- [70] N. C. Menicucci, Fault-tolerant measurement-based quantum computing with continuous-variable cluster states, *Physical review letters* **112**, 120504 (2014).
- [71] J. E. Bourassa, R. N. Alexander, M. Vasmer, A. Patil, I. Tzitrin, T. Matsuura, D. Su, B. Q. Baragiola, S. Guha, G. Dauphinais, *et al.*, Blueprint for a scalable photonic fault-tolerant quantum computer, *Quantum* **5**, 392 (2021).
- [72] C. F. Ockeloen-Korppi, T. T. Heikkilä, M. A. Sillanpää, and F. Massel, Theory of phase-mixing amplification in an optomechanical system, *Quantum Science and Technology* **2**, 035002 (2017).
- [73] K. Yosida, *Functional Analysis* (Springer-Verlag, 1980).
- [74] É. Gouzien, *Optique quantique multimode pour le traitement de l’information quantique*, Ph.D. thesis, Université Côte d’Azur (2019).
- [75] V. Yakubovich and V. Starzhinski, *Linear Differential Equations with Periodic Coefficients* (Wiley, New York, 1975) translated from Russian by D. Louvish.
- [76] D. Djoković, On the exponential map in classical lie groups, *Journal of Algebra* **64**, 76 (1980).